WIRELESS MONITORING OF RAILWAY EMBANKMENTS

A Thesis

by

VISHAL DANTAL

Submitted to the Office of Graduate Studies of
Texas A&M University
in partial fulfillment of the requirements for the degree of

MASTER OF SCIENCE

December 2009

Major Subject: Civil Engineering

WIRELESS MONITORING OF RAILWAY EMBANKMENTS

A Thesis

by

VISHAL DANTAL

Submitted to the Office of Graduate Studies of
Texas A&M University
in partial fulfillment of the requirements for the degree of

MASTER OF SCIENCE

Approved by:

Chair of Committee,	Charles Aubeny
Committee Members,	Robert L Lytton
	Zenon Medina-Cetina
Head of Department,	John Niedzwecki

December 2009

Major Subject: Civil Engineering

ABSTRACT

Wireless Monitoring of Railway Embankments.

(December 2009)

Vishal Dantal, B.E., Sadar Patel College of Engineering, Mumbai, India

Chair of Advisory Committee: Dr. Charles P. Aubeny

Landslides are one of the most dangerous geological hazards. In the United States, landslides cause a damage of $ 3.5 billion and kill 25 to 50 people annually. Shallow landslides occurring near any transportation facilities (railways and highways) can cause economic loss and disturbance of services which lead to indirect economic loss. It also increases the maintenance cost of those facilities. Hence, facilities located near a shallow landslide prone area should be monitored so as to avoid any catastrophic damages. Soil moisture and movement of the soil mass are prime indicators of potential shallow slide movements.

This assessment of wireless instruments considers a variety of devices ranging from devices for monitoring tilt and moisture at specific points in the soil mass to ground penetrating radar (GPR), which can give indications of moisture accumulation in soils over a wide spatial extent. For this assessment study, a low cost MEMS accelerometer was selected for measuring tilts and motions. And EC type soil moisture sensor was selected to measure soil moisture content of embankments. The instrumentation of

railway embankments works effectively and cheaply when a suspected problem area has already been identified and monitoring is needed over a limited spatial extent. This makes the monitoring system highly localized which often fails to cover potentially new failure prone areas. It is not feasible to use this approach to monitor soil conditions along the entire alignment of the railway. Therefore, another approach, GPR, is defined and explained in this study. GPR measures the dielectric constant value for any given material including soils. In soils, the dielectric constant value depends on the volumetric amount of water content present in a soil. Due to moisture infiltration, there is a reduction in suction value on embankment which indicates a decrease in shear strength of slope. Therefore, a correlation between suction and dielectric constant value is formulated in this study using Complex Refractive index model/Time propagation (CRIM/TP) model for soils. To validate this theoretical correlation, a laboratory study was conducted on pure kaolinite and on normal soil. For pure kaolinite this correlation proves beneficial while, for other type of soil, the correlation was off due to the limitations in filter paper test to measure suction below 2.5pF.

DEDICATION

To my parents and mentors who have guided me throughout my life and been there for me during the tough times.

ACKNOWLEDGEMENTS

I would like to thank Dr. Charles Aubeny for his guidance and help in the completion of the research. He showed me different ways to approach a problem and brought out the best in me.

I would like to express my profound gratitude to Dr. R.L. Lytton for teaching me the basics of this field and constant encouragement to do better. His expertise in this field made this research a success.

Thanks also to Dr. Zenon Medina-Cetina for being a member on my graduate committee.

I would also like to thank Hakan Sahin for helping me to perform filter paper test and other laboratory tests.

Finally, I would like to thank Deeyvid Saez and Michelle Bernhardt for helping me and supporting me throughout my research. I also like to thank my friends and colleagues and the faculty and staff for making my time at Texas A&M University a great experience.

TABLE OF CONTENTS

Page

LIST OF FIGURES

Page

Page

LIST OF TABLES

1. INTRODUCTION

Landslides can be described as downward movement of a part of slope by sliding, toppling or flow down the slope. Landslides mainly occur due to an extreme weather condition or due to a dynamic movement of tectonic plates. The major factor contributing to the occurrence of shallow landslides is heavy rainfall. The rainfall increases the soil water content and also raises the ground water table through infiltration; this causes to form a potential slip surface near ground water table and increase in pore water pressure contributes to decrease in shear strength between soil particles. This loss of shear strength in soil causes a failure of a slope. Landslides are one of the most dangerous geological hazards. In the United States, landslide causes a damage of $ 3.5 billion and kills between 25 and 50 people annually(Spiker and Gori 2003). Landslides can be distinguished in two different type of failure process.

1. Sudden failure due to extreme change in weather condition especially after heavy rainfall
2. Incipient failure of slope due to creep process

Sudden failure of any slope is due to extreme change in weather conditions like melting of a snow, heavy rainfall. These conditions increase the moisture content in upper 3 to 10 ft of soil layer.

This thesis follows the style of the *Journal of Geotechnical and Geoenvironmental Engineering.*

This variation of moisture decreases the shear friction between soils granular and shear strength of soil. The loss of shear strength can result into a sudden block failure or a debris flow.

Generally cohesive soil tends to fail as a sliding mass failure. As tension cracks develops in the initial stage of failure the wedge of soil mass becomes unstable and sliding force increases against the shear resistance between the soil mass causing failure of a slope (Fig. 1).

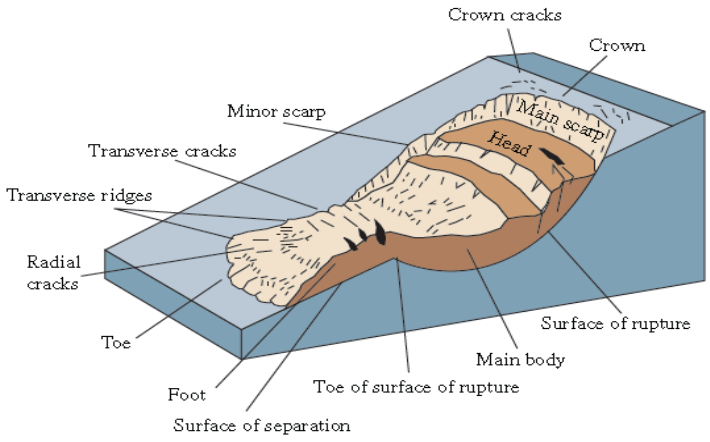

Fig. 1. Showing commonly used nomenclature for labeling the parts of landslides (Spiker and Gori 2003).

Shallow landslides occurring near any transportation facilities (railways and highways) can cause economic loss and disturbance of services which leads to indirect economic loss. They can also increase maintenance cost of those facilities. Hence facilities located near a shallow landslide prone area should be monitored so as to avoid

any catastrophic damages. Monitoring shallow slides involves, monitoring of soil moisture and movement of soil mass. These slides generally occur in remote locations, hence monitoring would lead to frequent site visits for data collection. These frequent site visits would increase the labor cost and overall operating cost for these systems. To avoid these drawbacks one can monitor slopes wirelessly from a control room, which will reduce the site visits and data can be acquired form system in real-time.

The current approach to monitoring railway tracks largely involves manual inspections which are a time consuming task. These inspection visits are mainly performed after any extreme weather condition occurs. The main drawbacks of manual inspection are as follows

1. The traditional point-by-point surveying and collecting data is very time consuming and laborious.
2. These observations are subjective, as they depend on inspector's experience.
3. The schedule for inspection is not defined properly; generally inspections are made after any extreme weather conditions.
4. Since observations are subjective, inspections should be performed by experienced personnel.

To overcome these drawbacks of manual inspections, a wireless monitoring of slopes is proposed in this thesis. Before deploying the wireless instruments to slopes prone to shallow landslides, an extensive site assessment will be done using GPR (Ground Penetrating Radar) to detect the sites with a high moisture contents or sites with

a high moisture variation which will increase the risk of shallow landslide. As GPR measures the dielectric constant for a given specimen, and the dielectric constant depends on the physical property of materials. Water has the highest dielectric constant value (ε=81). Therefore, a soil having high moisture content will have higher dielectric constant than a dry soil. This assessment of site can also give us an estimate of suction value for that site by know the engineering properties of soils and dielectric constant of soils in that site. The detailed explanation of these above mentioned techniques is done in following sections.

2. BACKGROUND

In recent years monitoring of slopes are based on different criteria and these monitoring systems where installed in known landslide prone areas. Monitoring of slides can be done by measuring the parameter which causes landslides. Such as predicting any failure from rainfall by modeling a rainfall intensity duration threshold models where the rainfall induced failure occurs frequently. This model can be expressed by the empirical formula to correlate rainfall intensity and duration of rainstorm.

$$I = 14.82\ D^{-0.39} \tag{1}$$

This is power law function was formulated by Caine (Caine 1980) after analyzing precipitation data for 73 failures of natural slopes. Where I is rainfall intensity (mm/hr) and D is the duration of precipitation in hours. The limit for rainstorm duration is more than 10 minutes and less than 10 days. This rainfall intensity duration modeling when combined with rainfall forecast and real-time rainfall measurement at particular site can form a basis for monitoring landslides and warning systems. For example, The Hong Kong Geotechnical engineering office has established a warning systems on the basis of rainfall intensity duration model and real time measurement of precipitation in 1977 for issuing warning signals for impending landslides (Chen and Lee 2003).

Another method of practice is to determine the geological deposits of soil. For example, the coastal bluffs between Seattle and Everett has sub horizontally bedded glacial and interglacial sediments with overlaying glaciolaustric silts deposits(Minard and Survey 1983). These sediments gets washed away and causes landslides during

heavy rainfall in this region(Baum et al. 2005). Hence it has become necessary to have hydrological monitoring to assess the landslides potential. The near real-time field data collection system were established at Edmonds and Everett where the data is normally collected in data logger at every hour in dry periods. When precipitation is high (>2.54 mm/hr) the reading is taken at 15 minute time intervals. These data were analyzed and provided on web server in form of graphs of soil wetness and precipitation. These graphs can be use to make correlation between rainfall intensity duration modeling and landslide activity.

Monitoring movements and soil moisture of slopes also plays important role to predict the landslide activity. The rate of movement of a surface can be used to predict the time of failure and using the soil moisture measurement one can predict the intensity of infiltration will cause instability of slopes.

The University of Wollongong Australia has monitored shallow slopes wirelessly at two different sites. In this real-time monitoring system, the cost of instruments was $(AUS) 18,000 in 2004 (Hungr 2005) excluding the cost of drilling and installation which depends upon number of hours and cost of labor. In this project, the slope named Site 355 was instrumented with In-Place Inclinometer and vibrating wire piezometer to monitor movements, and soil moisture sensors respectively. These instruments were connected to data logger CR10X of Campbell scientific to collect data and this data was transmitted through a cellular modem to office PC. This whole assembly was powered by 12 volt 7.ah(Amp hour) sealed lead acid batteries and these batteries were charged

through solar panels, the assembly of batteries and cellular modem was mounted on Campbell Scientific PS/12 power supply regulator unit. The data logger was programmed to record data at hourly basis in dry season and data were downloaded to an office PC on weekly basis. When the intensity of rainfall was high readings were taken at every 5 minutes interval and data was downloaded at 4 hours interval. These data can be accessed through a web server after analyzing it. This data was presented in graphs on a web server on its respective date of recording.

These monitoring systems are based on rainfall intensity thresholds for recording data from sensors. These types of monitoring systems are reliable for localized failure zone where the site conditions are assessed before deploying sensors. This site assessment is based on determining rainfall intensity for that site.

In this research study, a different type of preliminary site assessment is proposed which is using Ground Penetrating Radar (GPR). This preliminary site assessment is based on variation of soil moisture along the depth of slope which can be influenced by different parameters apart from rainfall intensity. Using this new type of preliminary site assessment will provide new failure zones which are influenced by different parameters.

3. WIRELESS INSTRUMENTATION OF SLOPES

3.1 Background

The adopted approach to monitoring of a landslide depends upon the mode of failure and cost of damage occurred due to failure. Landslides near the important facilities needs long-term monitoring programs to provide early warning of its failure to protect those facilities. While monitoring a landslide, certain parameters are taken to consideration, such as monitoring a groundwater level and movement of slope (Kane and Beck 2000). Apart from this, it is also important to monitor the variation of soil moisture of shallow slopes. Because most of the shallow failures occur during rainfall when there is a significant variation in soil moisture in upper 3ft to 10ft layer.

There are different types of instruments available commercially, depending upon monitoring parameters. Instruments such as piezometer are used to measure the variation of groundwater level, while extensometers, Inclinometers, tiltmeters are used to determine the rate of movement of soil mass and the direction of failure plane (Kane et al 2000). Apart from the selection of monitoring instruments, it is also important to determine the type of wireless data transmission system to be used. The selection criterion of data transmission system depends on power consumption, remote accessibility of site, currently available communication system, and cost of instrument and cost of operation. Most of these, wireless data transmission system works on IEEE 802.15.4 and zigbee transmission specifications (Garich 2007). The communication between the wireless sensor nodes and main server is done in three different ways; star,

peer-to-peer and hybrid topologies (Lynch and Loh 2006). Figure 2 shows three different types of topologies, and these are explained as follows: star topology, where transmission is to controller from different nodes and this type of topology limits the communications between others connecting nodes as they have to communicate through controller node. Peer-to-peer topology allows all nodes to communicate with each other and it also transfers data to controller through multiple and complex network. This complex array of network helps in sending data more reliably and quickly. It also allows for self healing and self organizing the network to connect with controller. But this type of topology consumes more power to transmit data to controller. Lastly, the hybrid topology incorporates both star and peer-to peer topologies to transmit data efficiently with consuming less power (Lynch and Loh 2006).

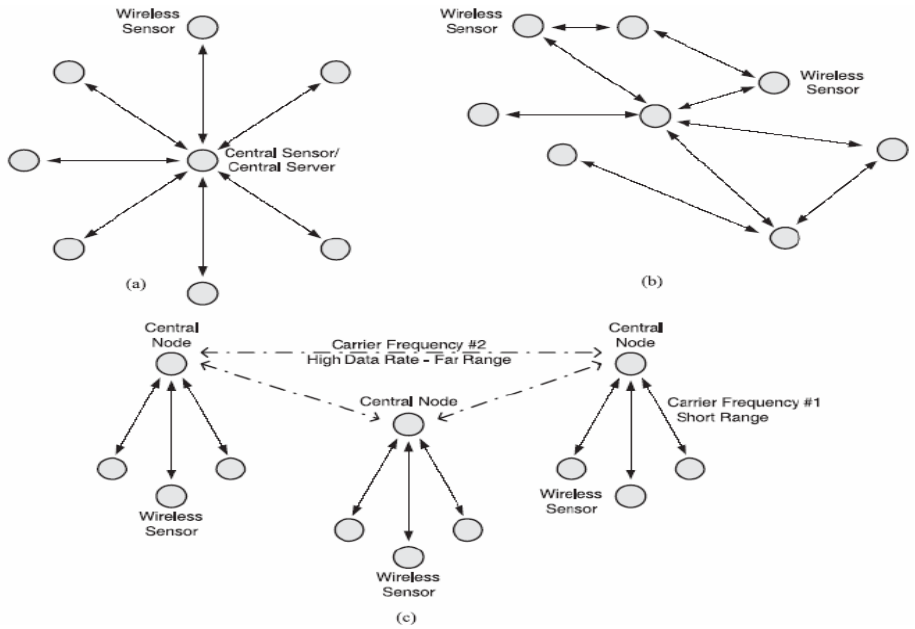

Fig. 2. Common network topologies for wireless sensor monitoring networks: (a) Star, (b) Peer-to-peer or mesh, (c) Hybrid(Lynch and Loh 2006).

Alternatively, the data acquisition can be done using an onsite data logger and then sending this data wirelessly to main server using cell phone network at specific time intervals. At the same time it can be programmed for data sampling depending upon the rate of change of readings (Kane and Beck 2000).

3.2 Monitoring the Influencing Parameters

In this monitoring system we will be monitoring different parameters such as

1. Monitoring soil water content/suction pressure
2. Measuring surface movement
3. Monitoring deformation profile along the depth.

Measuring soil water content and suction pressure is essential to monitoring any potential landslides. As most major shallow surface failure occurs after heavy rainfall, it becomes necessary to know the effects of water content on soil suction, as suction is a major contributor to soil strength. When moisture infiltration occurs, suction can decline to values as low as about 2 pF. Depending on the slope angle and the depth of moisture penetration, slope instability becomes highly at this low level of suction(Aubeny and Lytton 2004). As the soil moisture increases it increases pore water pressure in between soil particle and decreases contact friction between soil particle which leads to loss of shear strength and block of mass slides at critical plane causes failure of slope.

Measurement of surface movement can be used to predict an incipient landslide by measuring the rate of movement of surface. If the rate of movement increases, a

warning signal will be transmitted. Monitoring surface movement would help us to monitor creep motion of slope and the increase in rate of creep motion can be used to predict the incipient failure of slope.

3.2.1 Use of instruments for monitoring slopes

For monitoring any kind of slope deformation it is important to have information on slope movements as well as any other relevant factors related to a potential slide. The slope movement can be measured using different types of measurement methods which are as follows.

3.2.1.1 Accelerometers as motion sensor

An accelerometer is a device which measures acceleration and forces induced by gravity with its vector direction(Hoffman et al. 2006). These systems are mainly used as sensors to monitor a different process. Micro-Electro-Mechanical Systems MEMS Accelerometers are one of the simplest MEMS and most of the common low cost MEMS. Accelerometers work on the concept of a differential capacitance to detect the acceleration of an object to which it is attached.

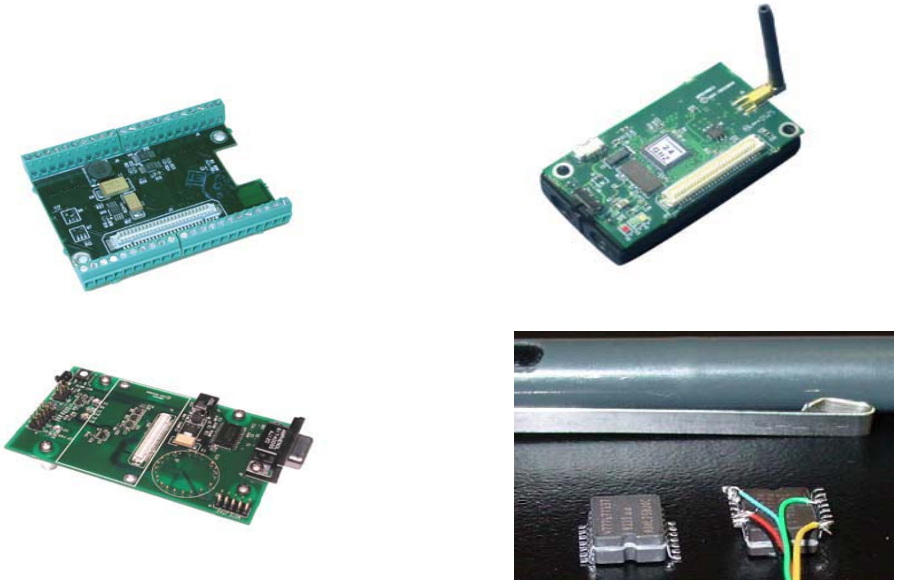

Fig. 3. (Clockwise from bottom left) MIB510 gateway board,MDA300 data acquisition board,MPR2400 wireless transmission board(Crossbow Technology 2008),MEMS accelerometer and wire connection (Hoffman et al. 2006).

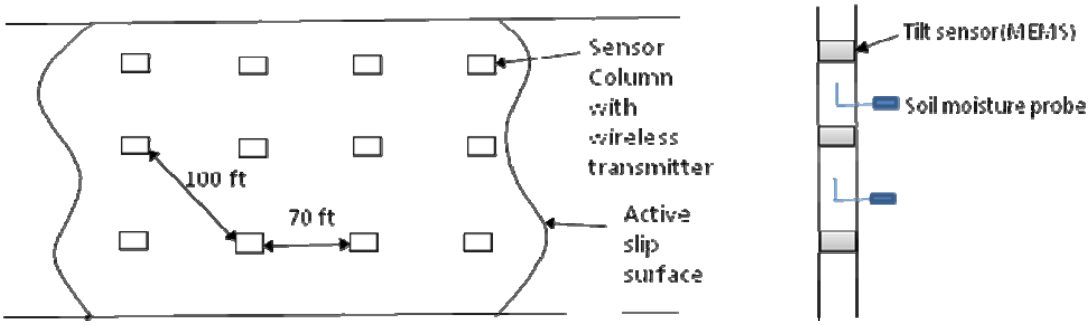

Fig. 4. A proposed layout of sensor columns and components of a sensor column.

Installation of MEMS for measurement of tilt can be done as follows

- Accelerometer has to be encased in water tight tube and proper connection should be made with wireless transmitter (Fig. 3).
- A flexible casing can be provided around these sensor tubes to protect it from sudden failure of sensors (Fig. 4).
- A proper spacing should be determined between sensors in a sensor tube.
- For measuring a lateral movement of surface a reference point has to be established outside the active movement area of slope.
- To determine a slip surface of a slope, a sensor tube should be drilled down up to a depth of stable zone.
- For maximum strength of wireless signals, transmitters should be placed at least at a maximum spacing of 100ft (Fig. 4).

3.2.1.2 TDR (Time Domain Reflectometry) as motion sensor

TDR is widely used in detecting fault or breaks in coaxial cables. In this method an electric pulse is transmitted along the length of cable from cable tester and, if some breaks or deformation occur at a given location , part of voltage is reflected back to cable tester that records the voltage change (spikes) with respect to depth of cable (Kane et al. 2001). The correlation can be made between the measured voltage spike and cable deformation. This mechanism can be used for monitoring slope movements. By this method a cable is installed to a depth located in the stable zone of the soil mass. It is

surrounded by brittle cement grout so that large movements of the soil will the break grout and deforms the cable which can be by the cable testers (Fig. 5).

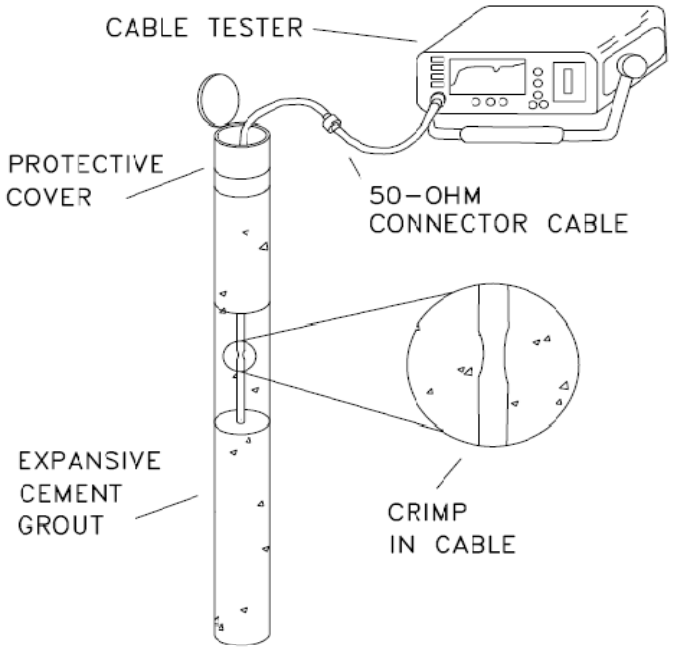

Fig 5. Schematic of cable installation and monitoring (Dowding and O Connor 2000).

- Datalogger

It is used to store data recorded by cable tester and it can be programmed to do certain steps such as to turn on cell phone modem or cable tester(Kane and Beck 2000) and to record voltage values of cable from cable tester it has own inbuilt memory to store up all these data and a processor to execute certain tasks.

- Multiplexer

Multiplexer is device in which we can connect multiple sensors or cable and this multiplexer is connected between cables and datalogger. Data collected by datalogger in a sequential manner from each cable through switches of multiplexer (Kane and Beck 2000). A multiplexer can be attached to another multiplexer to take readings of large network of cables.

- Power

Usually this system requires more power and it also depends on numbers of instruments attached to a system. Typically for small system have two or three sensors and a cell phone require small rechargeable gel-type battery. Power for large networks of cables, cable tester and cell phone can be provided by a larger battery at least of 12V rechargeable battery and this battery can be recharged by solar panels.

- Communication

A reliable and clear communication is required between datalogger and remote server. Generally a hardwire telephone connection is most reliable but for remote terrain a cell phone can be used and in addition of these it also requires a modem to communicate.

Field deployment

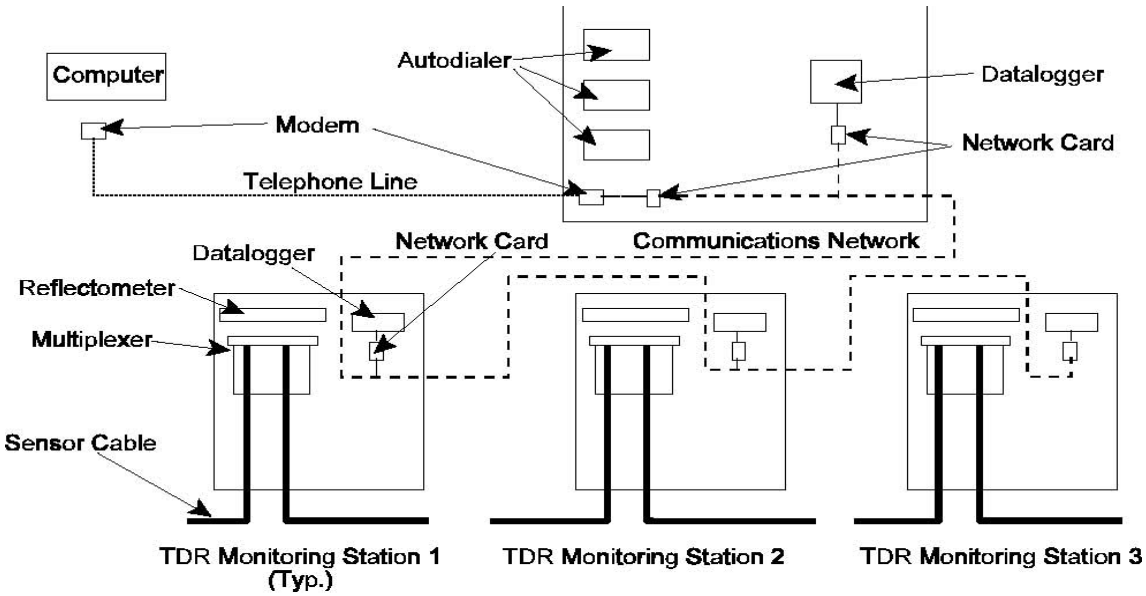

Fig. 6. Central control and monitoring unit schematic (Kane and Beck 2000).

Installation of TDR can be done for two purposes, first it can be used to determine the location of the failure surface and secondly it can be used to monitor shallow slope slides.

For determining failure surface the installation of TDR is as follows

- A borehole has to be drilled up to the stable zone and it can be done by using CPT driller.
- A coaxial cable is to inserted in that hole and cable is anchored by brittle grout(Kane et al. 2001). If there is any movement then it will break the grout and cable will show some deformations.

- Now the cable is connected to cable tester which generates a high voltage pulse and passes through cable, any deformations will be identified by the cable tester.
- To do this process wirelessly a data logger and wireless modem can be attached to this testing module (Fig. 6).

3.2.1.3 In- Place inclinometers as motion sensor

Inclinometers are generally used to measure tilt and to monitor lateral movements for embankments and dams. It consists of Inclinometer casing, electrolytic inclination sensors, strings connecting sensors and guide wheels (Fig. 7).

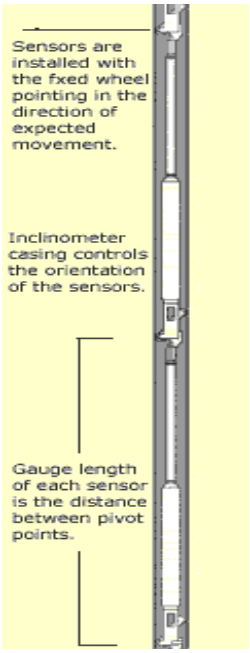

Fig. 7. Components of In-Place Inclinometer(Slope Indicator 2006).

The field deployment is laborious process in this system. A borehole is drilled down to the estimated depth of the stable zone and a casing is inserted. The casing is then checked for verticality by spiral sensors. Finally, an electro level (EL) In-Place Inclinometer is lowered down with the series of Inclinometers is connected to a data logger.

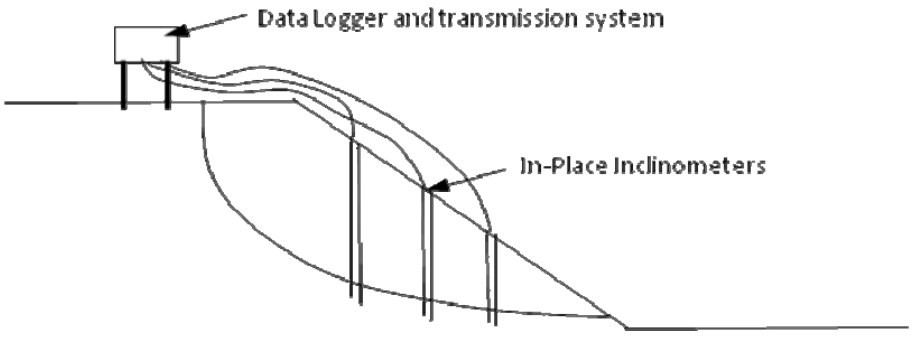

Fig. 8. Schematic for installation of In-Place Inclinometers.

Field deployment

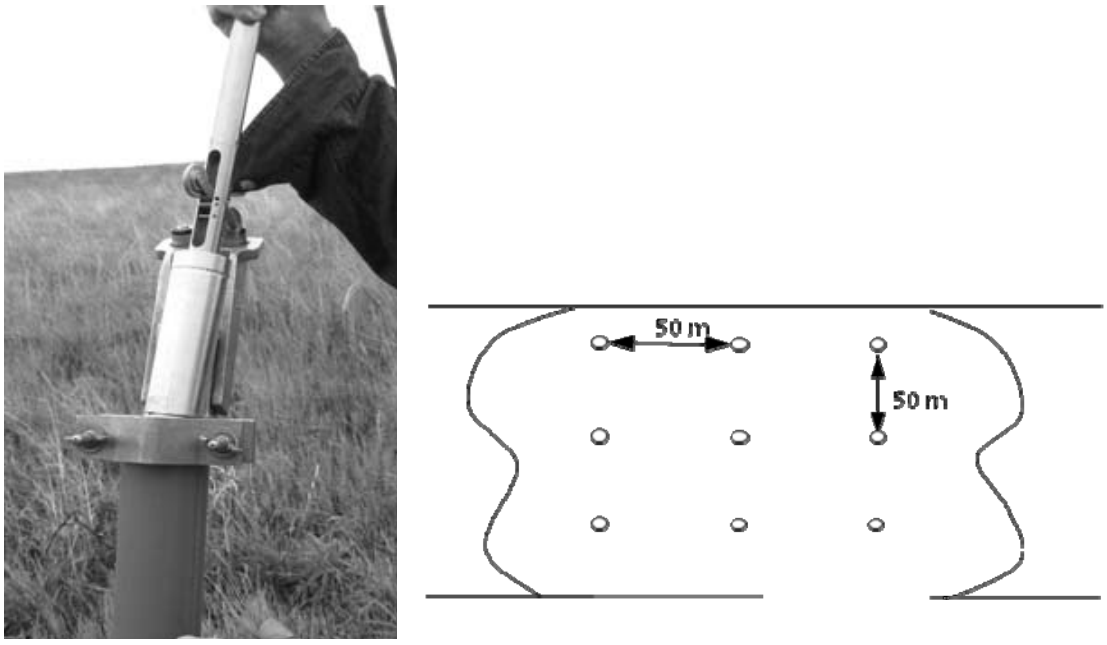

Fig. 9. Installation of In-Place Inclinometer(Furlani et al. 2005) and layout of In-Place Inclinometers in active surface(Plan view).

- A borehole is drilled using CPT borehole driller and a flexible spiral casing is inserted up to a depth of stable zone (Fig. 8).
- The verticality of casing has to be checked and if corrections are required to the reading the it has to be determined, verticality is checked by running spiral sensors throughout the casing.(Dowding and O Connor 2000).
- An In-Place Inclinometers are placed in series along the depth of casing all these Inclinometers are connected to data logger.

- As each Inclinometer requires one data logger this can be reduced by connecting multiplexer between Inclinometer and data logger up to ten Inclinometers can be attached to one multiplexer and this can be used between two boreholes (Fig. 9).
- Data logger is then connected to wireless modem to transfer data via using cell phone device to main sever.

3.2.1.4 Water content sensor

Soil water content is essential factor for predicting slope failure (Baum et al. 2000) and monitoring of this parameter is as important as monitoring slope movement. Instruments measuring soil water content are mainly used in agricultural sector to monitor optimum soil moisture of crops and for irrigation purpose. These instruments are commercially available which can be used for slope monitoring purpose along with movement measurement devices. This sensor works on principle of measuring dielectric constant of soil to find out the water content of soil in which it is buried.

There are different types of sensors available to measure soil water content based on its working principle. The most common low cost sensor is ECH2O sensor (Decagon Devices 2008a) (Fig. 10) which works on measuring dielectric constant of soil to determine soil water content and the difference in voltage output can be directly co-related to volumetric soil water content. These sensors can be attached to any type of system such as it can be connected to data logger or to any data acquisition board to collect data wirelessly.

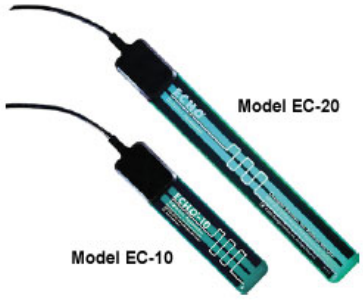

Fig. 10. Soil moisture sensors (Decagon Devices 2008a).

3.2.1.5 Use of tensiometer for suction measurement

Soil suction plays important role in determining the stability of slope in high plastic clays where change in suction due to climate variation plays influencing factor for shallow slope failure. Soil suction is measured by tensiometers which are low-cost and commercially available (Fig. 11). These sensors works on accurate pressure transducer connected in ceramic cup where water pressure produces analog signal to read difference of electric pulse to determine suction pressure of water in soil particle.

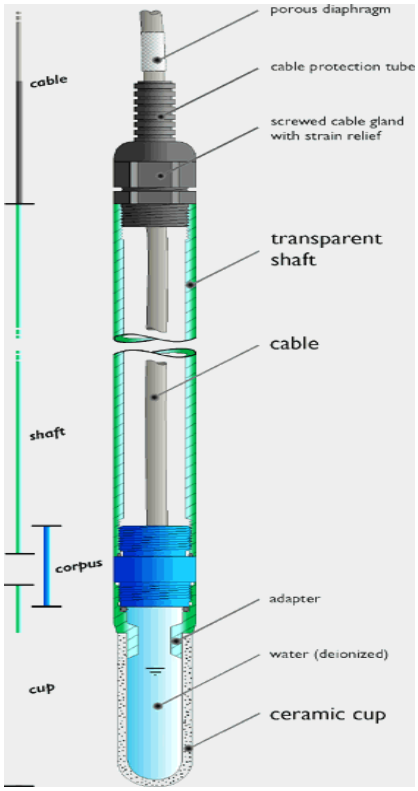

Fig.11. T4 tensiometers for measuring soil suction sensor (Decagon Devices 2008b).

This low maintenance sensor works on a soil water tension in ceramic cup is transmitted into tensiometer. The range of measuring suction is -1000 to 850 hPa (approx 2.9 pF) and consumes 1.3 mA at 10.6 V.

3.3 Suction Model for Infiltration of Moisture on Slopes

3.3.1 Background

Suction is defined as an ability to attract and retain water in pores of porous materials such as soils. It is measured as a negative stress in pore water. The soil suction

is consists of two components; matric suction and osmotic suction. The sum of these two components is total suction. Matric suction is mainly due to capillarity, texture and surface adsorption. Osmotic suction is due to dissolved salts contained in the soil water. The equation for total suction is as follows.

$$h_t = h_m + h_\pi \tag{2}$$

where,

h_t= total suction (kPa)

h_m= matric suction (kPa)

h_π= osmotic suction (kPa)

Using the principles of thermodynamics, total suction can be expressed in Kelvin's equation derived from ideal gas law,

$$h_t = \frac{RT}{V} \ln\left(\frac{P}{P_o}\right) \tag{3}$$

R= universal gas constant

T= absolute temperature

V= molecular volume of water

P/P_o = relative humidity

Matric suction can be obtained by calculating a difference in pressure between the applied air pressure and water pressure across a porous plate in a pressure plate apparatus or in a pressure membrane device. Matric suction can be expressed as

$$h_m = -(u_a - u_w) \tag{4}$$

There are salts dissolved in the water present in the soil. The water vapor pressure of solvent is lesser than that of pure water. Therefore, the relative humidity decreases with increasing concentration of salts (Fredlund and Rahardjo 1993). The osmotic suction is due to these dissolved salts in the pore water of the soil sample. It is related to the tendency of water to move from the region of low salt concentration to high concentration. The changes in osmotic suction affect on the mechanical behavior of the soil i.e. changes in volume and shear strength occur (Fredlund and Rahardjo 1993).

3.3.2 Suction model

The strength of shallow slopes of high plastic clays is mainly derived from negative pore pressure (matric suction) and angle of internal friction between soil particles. It also depends on angle of slope and moisture infiltration on surface of slope. But majority of strength in high plastic clays is due to presence of high negative pore pressure in top layer of slope. In this section, a stability model is coupled with suction moisture envelope to characterize the strength of shallow slopes. Furthermore, a factor of safety is evaluated at different depths for different governing criteria (Fig. 12).

The strength in compacted soils is mainly due to internal strength and matric suction. In compacted soils the cohesion is destroyed during compaction and therefore does not contribute in shear strength for these soils. In this case, the shear resistance is characterized using generalized Mohr- coulomb equation for an unsaturated soil(Fredlund and Rahardjo 1993).

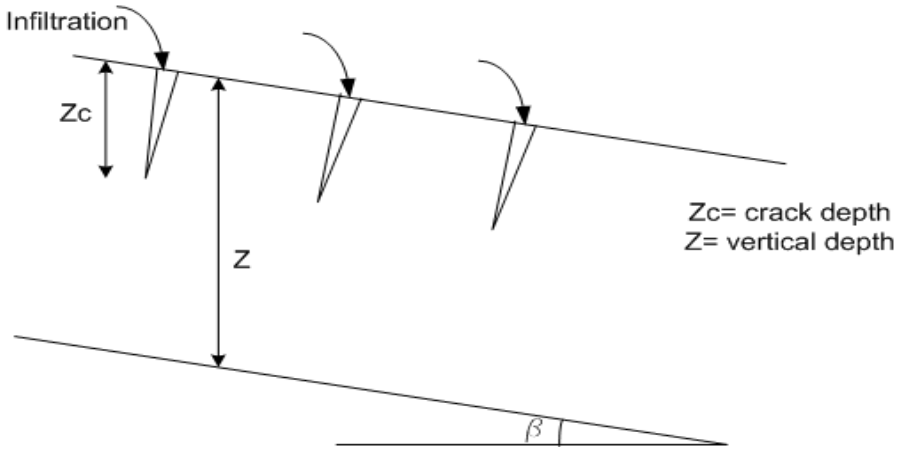

Fig. 12. Schematic diagram for moisture infiltration on slope with cracks on its surface.

$$\tau_f = (\sigma_n - u_a)\tan\phi' + f\theta(u_a - u_w)\tan\phi' \tag{5}$$

As the moisture infiltrates, this equation tends to saturation state and there is some increases in pore water pressure due to shear resistance which is discussed later in this section.

$$\tau_f = (\sigma_n - u_w)\tan\phi' \tag{6}$$

In above all equations cohesion is considered as zero. Where τ_f= ultimate shear resistance; (σ_n-u_a) =net mechanical stress normal to failure plane defined as the difference between total overburden stress σ_n and the pore-air pressure u_a; (u_a-u_w) =the difference between pore-air pressure u_a and porewater pressure u_w; f'=effective friction angle; θ=volumetric water content=volume water/total volume; and f=factor ranging from 1/θ to 1 depending on degree of saturation.

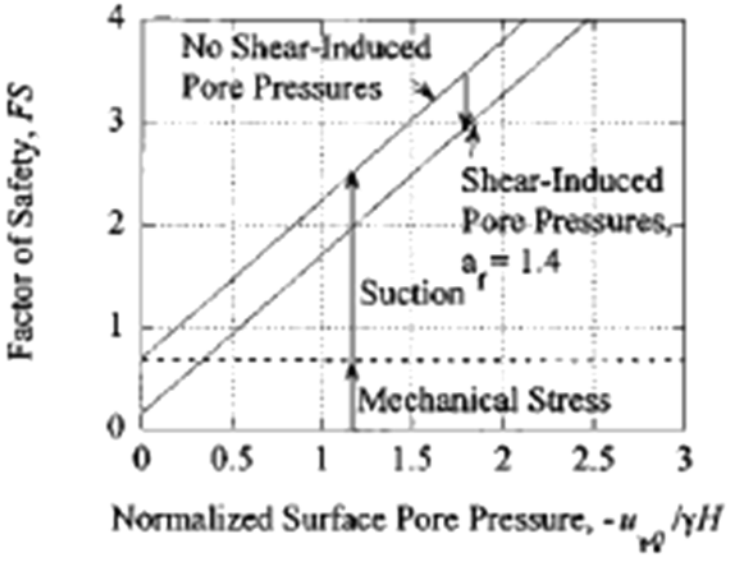

Fig. 13. Contributions of mechanical stress and suction to stability for a 3H:1V slope with ϕ'=25°(Aubeny and Lytton 2004).

During failure of potential slide mass there is an increase in pore water pressure which is termed shear induced pore water pressure (Fig. 13). This increase in pore water pressure occurs just before the failure of the slide mass. Hence it is appropriate to

consider undrained or partially drained conditions of shear during failure. The increase in pore pressure can be explained using the Henkel parameter a relating shear induced pore pressures Δp_s to octahedral shear stress $\Delta\tau_{oct}$(Holtz and Kovacs 1981). Therefore the shear induced pore pressure is $\Delta u_s = a\sqrt{2/3}\Delta\tau$. Apart from this, there will be constant pressure head due to moisture infiltration above the sliding mass which will contribute towards the pore pressure. Secondly, a constant initial suction pressure will be considered as the surface of the slope is exposed to uniform atmospheric conditions and this suction includes the uniform osmotic suction. The equation for pore water pressure can be expressed as follows

$$u_w = u_{w0} + \gamma H \cos^2\beta + \sqrt{2/3}a\gamma H \sin\beta\cos\beta\,. \tag{7}$$

The final shear resisting equation for a given potential slide mass is expressed as

$$\tau_f = c' + (\gamma_t z\cos^2\beta - u_{w0} - \sqrt{\frac{2}{3}}a_f\gamma_t z\sin\beta\cos\beta)\tan\phi'\,. \tag{8}$$

The driving force for a potential slide mass is expressed as given below. Considering the fact that failure plane is parallel to the surface of slope and it is considered infinite in a lateral direction.

$$\tau_{au} = \gamma_t z\sin\beta\cos\beta\,. \tag{9}$$

Factor of safety is defined as ratio of resisting force over driving force. Therefore, factor of safety for a potential slide mass with above explained criteria is expressed as follows

$$FS = \frac{(\gamma_t z \cos^2 \beta - u_{w0} - \sqrt{\frac{2}{3}} a_f \gamma_t z \sin \beta \cos \beta) \tan \phi'}{\gamma_t z \sin \beta \cos \beta} \tag{10}$$

Using above equations, a code is written in a Matlab® to find out the governing parameters for above equations. Along with this, a suction pressure is evaluated across the depth of slope using suction- moisture envelope (Fig. 14).

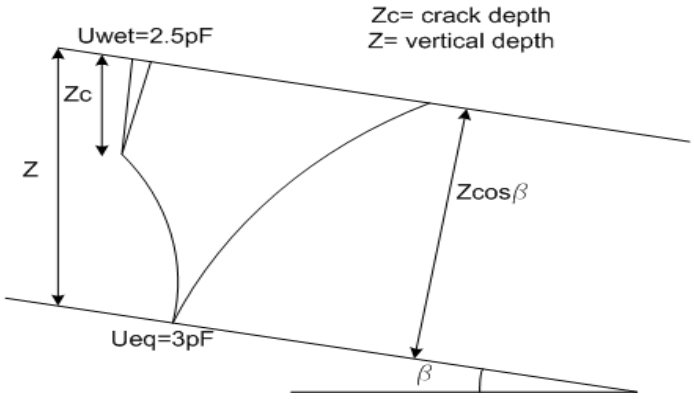

Fig. 14. Suction profile for a slope with a crack depth.

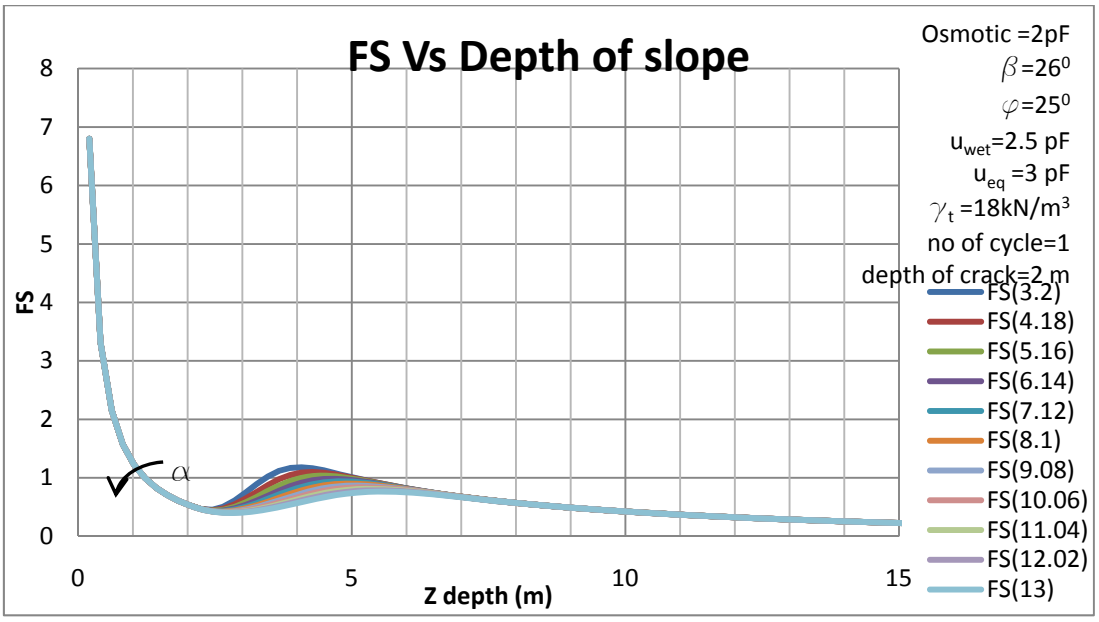

Fig. 15. Factor safety versus depth of slope chart with different moisture diffusion coefficients at slope angle =26^0.

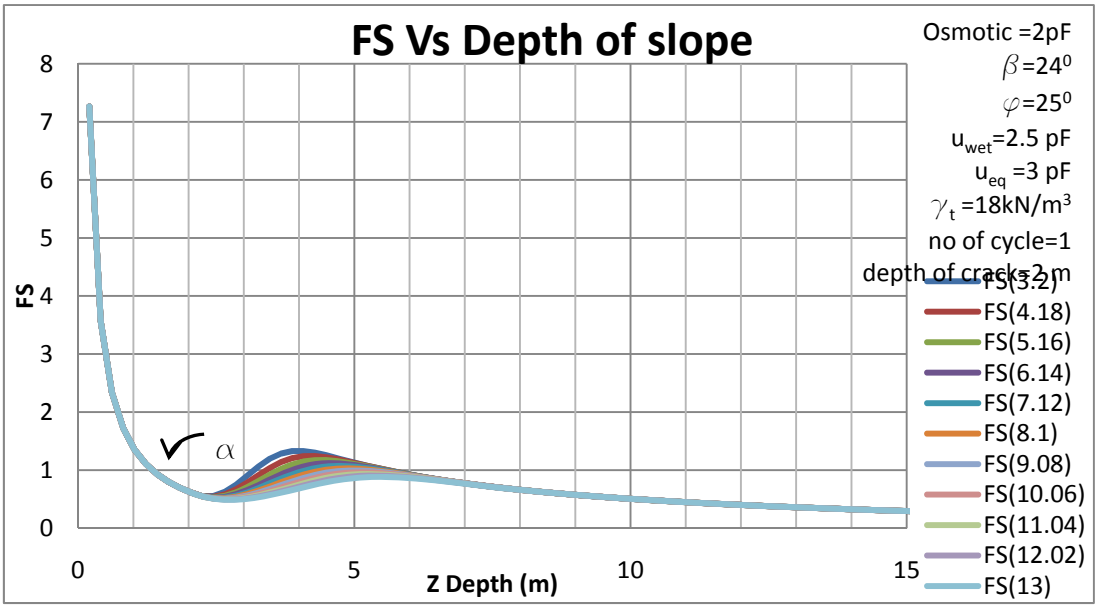

Fig. 16. Factor safety versus depth of slope chart with different moisture diffusion coefficients at slope angle =24^0.

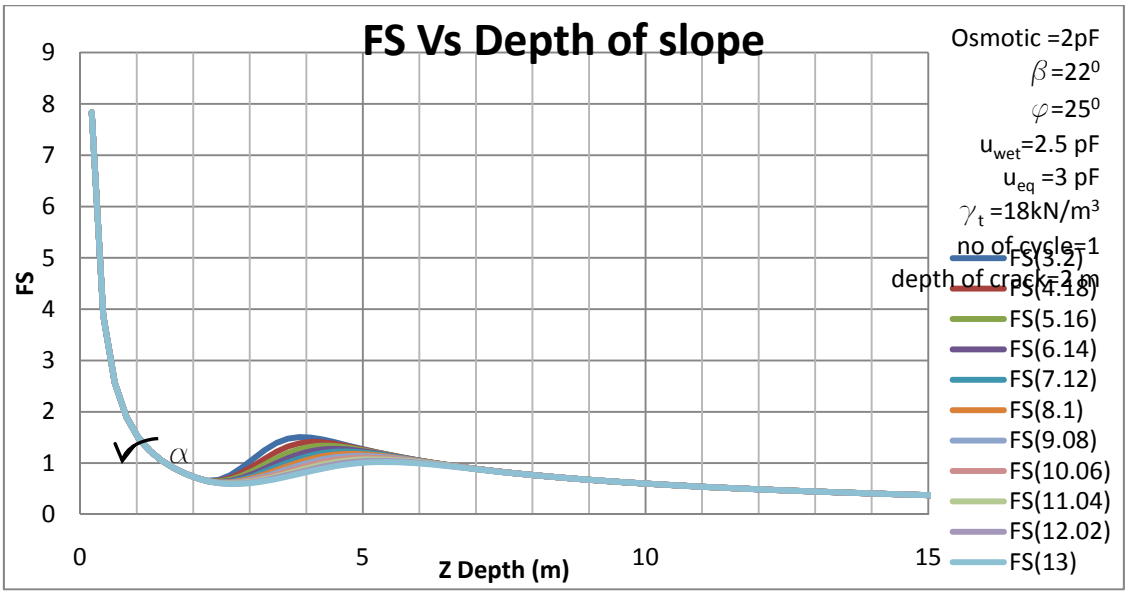

Fig. 17. Factor safety versus depth of slope chart with different moisture diffusion coefficients at slope angle =22^0.

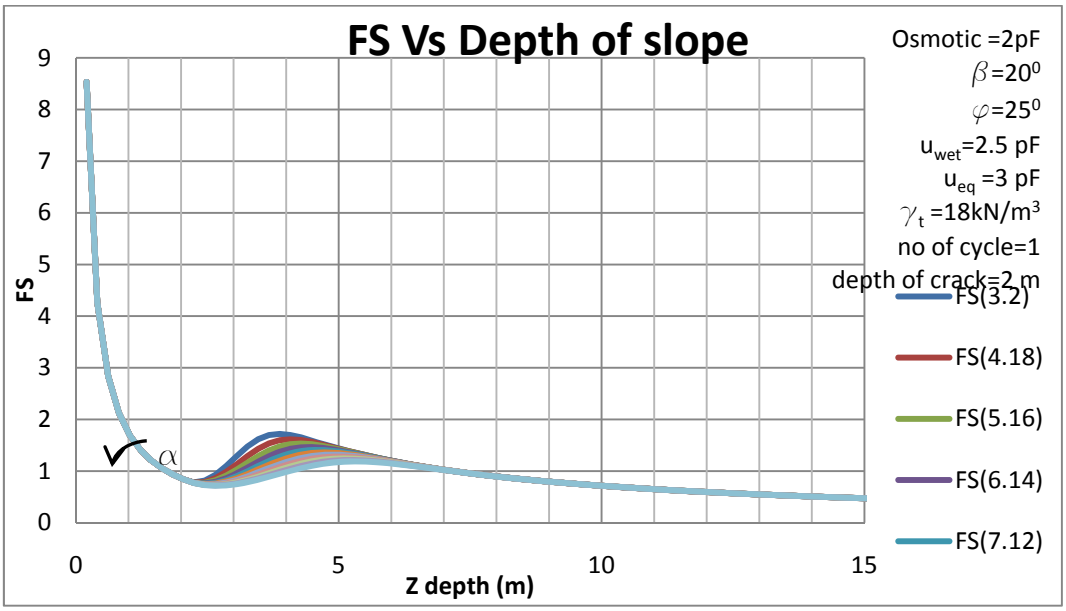

Fig. 18. Factor safety versus depth of slope chart with different moisture diffusion coefficients at slope angle =20^0.

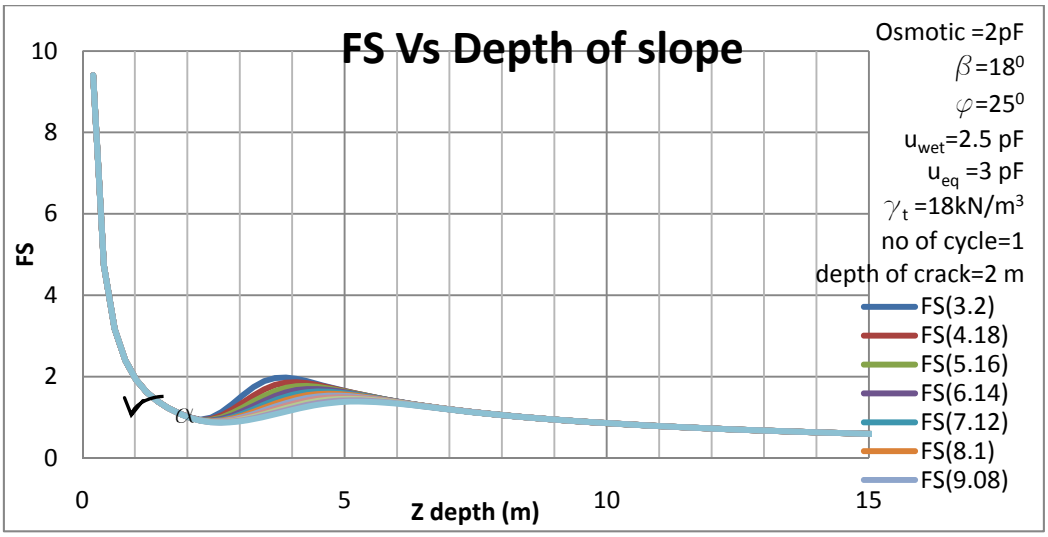

Fig. 19. Factor safety versus depth of slope chart with different moisture diffusion coefficients at slope angle $=18^0$.

The above parametric study for shallow slopes shows that the factor of safety is governed by coefficient of moisture diffusion, angle of slope, depth of cracks, number of wetting and drying cycles (Fig. 15 to Fig. 19). Of these parameters, the most significant ones are depth of cracking and coefficient of moisture diffusion. It shows that, as the depth of cracks are in between 1m to 2m of slope it reduces the factor of safety drastically in that region and it regains back to factor of safety of 1 after 4m of depth depending upon the angle of slope. And, most of the shallow slope failure occurs in first 3m of depth of slope. Apart from the depth of cracks, the Factor of safety also changes significantly with the change in moisture diffusion and angle of slope. Higher the coefficients of moisture diffusion lower the value of factor of safety after depth of cracks, and higher the angle of slope lower the regain value of factor of safety after depth of cracks.

3.4 Assessment for Potential Use of Wireless Instruments as Monitoring Systems

For any wireless instruments to use as monitoring systems should have following basic requirements:

- Low Cost
- Low maintenance
- Expandable for future technology
- Work efficiently during extreme weather conditions
- Low power consumption

Based upon these criteria above mention instruments are assessed for monitoring systems.

1. Using an accelerometer as a tiltmeter and soil moisture sensor for water content measurement

Accelerometer measures acceleration and force induced by gravity with its vector direction (Hoffman et al 2006). The accelerometer works on principle of MEMS which measures the differential capacitance to detect induced force. This is one of the low cost MEMS available and it is widely used in measuring vibrations and dynamic loadings on buildings and on bridges. The average costs of this instrument are in between $8.00 to $35.00. Being a low cost instrument it can be used as a monitoring device and the maintenance for this instrument is also low. Since it works on basic principle, this instrument is also compatible with new technology. When encased in water resistant, air

tight containers, this instrument works efficiently in any extreme weather conditions. Power requirements are low and the device can be attached to solar powered batteries to operate as monitoring device.

To measure the soil water content, a soil moisture sensor can be used along with the accelerometer. The power consumption is also low as compared to accelerometers. The maximum current consumption for this device is 2.5VDC (Volt direct current) which can be supplied by solar powered batteries. These two instruments can be connected to any data acquisition board to collect data. This setup can be connected to wireless transmission board to transmit data wirelessly. The single data transmission and acquisition board can be attached to series of sensors along the depth of slope to form a sensor column. The average cost of this sensor column comes around $620.00 for each sensor column excluding the cost of drilling, casing and wiring. Since the cost of instruments is less, the total cost for this type of monitoring system depends on cost of installation.

2. Use of TDR as a deformation sensor and soil moisture sensor for soil water content

The TDR (Time Domain Reflectometry) works on a simple method of transmitting electric pulse and receiving it. And the time difference is recorded between transmitting and receiving of electric pulse. This difference in time is used to detect breaks and faults in that cable. This instrument can be used for slope monitoring to detect the slip surface of a given slope. This instrument needs a cable tester which

generates electric pulse; therefore it consumes more power than an accelerometer. It also requires traditional data loggers which consume more power than a wireless data acquisition board. The power consumption for these data loggers is around 12V which can be recharged through solar panels. Apart from this, the data logger should be placed on firm ground and far away from active zone. Soil moisture sensors can be installed separately from the TDR but they can be connected to same data logger.

The overall cost of this type of sensors mainly depends on cable tester, data logger and cost of installation. The cables are installed in low strength cement grout to keep cables vertical and to avoid false readings. The total cost for this instrument is around $3455.0 excluding cost of installation and grouting.

3. Use of traditional In-Place Inclinometers as a tilt sensor and soil moisture sensor for water content measurement.

In-Place Inclinometers are generally used to measure tilt and lateral movements in dams and embankments. These instruments are expensive as compared to the accelerometers. This instrument also needs a data logger and a casing to install along the slope. The casing for this instrument should be perfectly vertical and this can be checked by running a spiral sensor inside the casing (Dowding and O Connor 2000). The power consumption for this sensor depends upon type of Inclinometer is used and type of data logger is used. Power requirement for a Campbell scientific data logger is 12V and this can be supplied by a solar panel charged rechargeable gel-type battery. Soil moisture sensors can be installed along with these Inclinometers on the same data logger. The cost

of these sensors depends on cost of installation and the total number of Inclinometers is used. The average cost for this type of sensor is $3455.00 (Campbell Scientific 2008) excluding the cost of installation and the cost Inclinometers.

Considering the same cost of installation for all these above mentioned instruments, the cost for an accelerometer as a tiltmeter comes out to be less expensive than the TDR and Inclinometer. The cost of maintenance is also low for these accelerometers. Therefore the combination of accelerometer and soil moisture sensor is much cheaper than any other combination.

4. GROUND PENETRATING RADAR

4.1 Introduction

4.1.1 Ground penetrating radar

The GPR (Ground penetrating radar) works on similar principles of sonar technique. The radar emits a high- frequency electromagnetic waves (10-1000 MHz).This wave travels through soil from sources antenna and wave is received by receiver. The propagation and reflection of wave mainly depends on the dielectric permittivity of soil, which is strongly related to soil water content (SWC)(Topp et al. 1980). Any subsurface contrast in dielectric properties will reflect part of the wave energy back to the surface. The reflected wave is detected by the receiving antenna as a function of time. These radar signals are influenced by the high frequency electrical properties of ground(Davis and Annan 1989). The electrical properties of soils depend on the water content in that soil. This change in electrical properties causes radar signals to partly reflect and partly transmit through the soil. The reflection is from the surface where change in electrical property occurs. Hence, it gives the profile of soil layers and the zone of high water content in soil. The commercially available time domain GPR has three different modes which can be used for profiling soil. These modes are common midpoint (CMP), wide–angle reflection and refraction (WARR), and transillumination (Fig. 20).

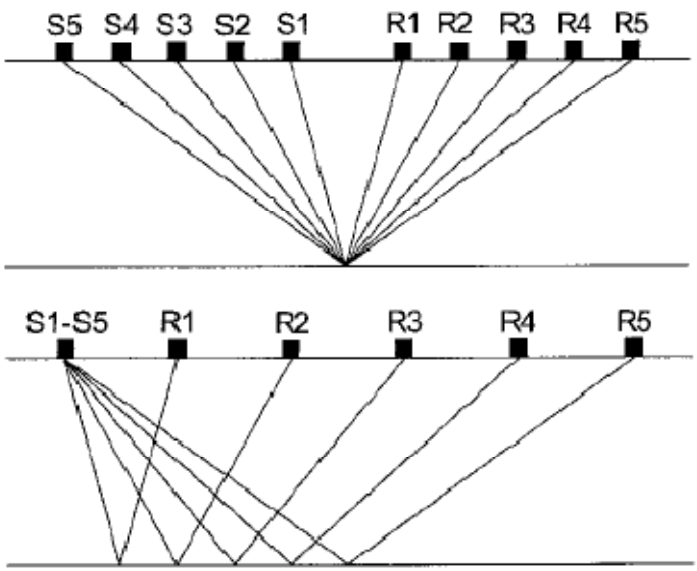

Fig. 20. Common-midpoint (CMP, top) and wide angle reflection and refraction (WARR, bottom) acquisition, where S denotes the transmitter location and R denotes the receiver locations.(Huisman et al. 2003).

4.1.2 Electrical properties for different soils

The electrical properties of soils are governed by different parameters such as magnetic susceptibility and dielectric permittivity. This dielectric permittivity has prime importance for detecting soil moisture content. The dielectric permittivity is a complex number and is a function of frequency. The ratio of complex dielectric permittivity to free space dielectric permittivity (dielectric permittivity of air) is called as relative dielectric permittivity.

$$K^*(\omega) = K'(\omega) - iK''(\omega) \tag{11}$$

where K* is relative dielectric permittivity

K' is real part of dielectric permittivity

K'' is imaginary part of dielectric permittivity

ω is frequency (Hoekstra and Delaney 1974)

The real part of dielectric permittivity can vary from 1 for air to 81(for free polar water at 20^0C) in a given natural soil sample (Table 1.). In soil dielectric permittivity of water depends on degree of bonding of water molecules around soil particles (Dobson et al. 1985).

4.1.3 Relation between dielectric permittivity and soil water content

The relationship between dielectric permittivity and soil water content which was proposed by Topp et.al 1980 is widely used to relate GPR measurements with soil water content for given site. The empirical formula for mineral soils is given as

$$\theta = -5.3\times10^{-2} + 2.92\times10^{-2}\varepsilon - 5.5\times10^{-4}\varepsilon^2 + 4.3\times10^{-6}\varepsilon^3 \quad (12)$$

where θ = volumetric water content

ε= dielectric permittivity of a sample.

Table 1. Typical electromagnetic properties of selected material (Morey 1998).

Material	Relative Dielectric Constant, ε_r	Electrical Conductivity (mS/m)	Velocity (m/ns), v	Attenuation (dB/m), A
Air	1	0	0.30	0
Fresh Water	81	0.05	0.033	0.1
Sea Water	80	$3x10^4$	0.015	10^3
Dry Sand	3–5	0.01	0.15	0.01
Saturated Sand	20–30	0.1–1.0	0.06	0.03–0.3
Silts	5–30	1–100	0.07	1–100
Clays	5–40	2–1000	0.06	1–300
Limestone	4–8	0.5–2	1.12	0.4–1
Granite	4–6	0.01–1	0.13	0.01–1
Bituminous Concrete	3–6	0.5–1.5	0.12	0.05–0.5
Concrete (cured)	6–11	1–3	10	0.5-1.5

4.1.4 Measuring soil water content using ground wave signals

The ground wave signals are the waves traveled through soil layer. The strength of this wave depends on separation distance between antennas, and the frequency of the GPR signal. Figure 21 shown below illustrates the type of waves can be received from GPR signal.

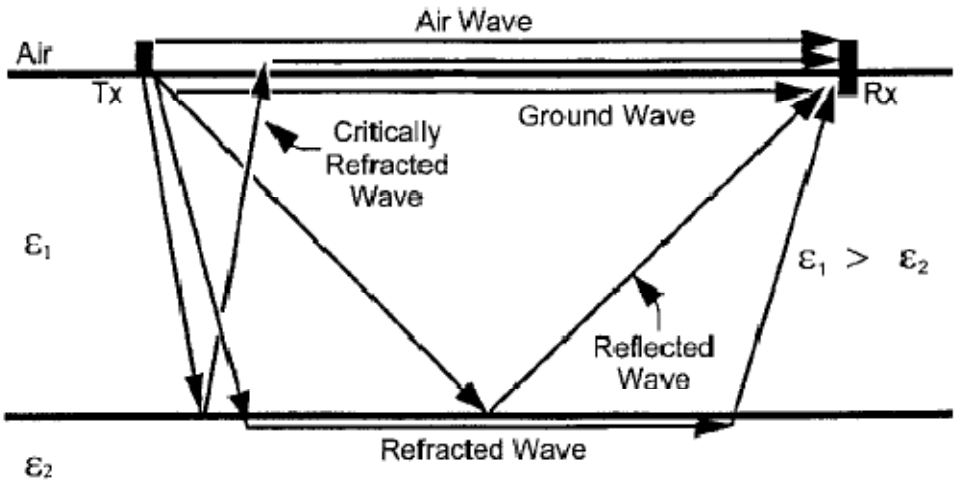

Fig. 21. Propagation paths of electromagnetic waves in a soil with two layers of contrasting dielectric permittivity (ε_1 and ε_2) (Huisman et al. 2001).

Using the wide angle reflective and refractive (WARR) mode for receiving wave's one can directly correlate slope of ground wave to the ground wave velocity. This ground wave velocity can be used to determine the water content for given surface. According to (Huisman et al. 2001) a proposed procedure for determining the soil water content using ground wave of GPR(Fig. 21):

1. Identify an approximate ground wave arrival time for different antenna separations in a multi-offset GPR measurement,
2. Choose an antenna separation where the ground wave is clearly distinguished from the air and reflected waves and
3. Use this separation of antenna for GPR measurement to relate the changes in ground wave arrival time to change in soil permittivity.

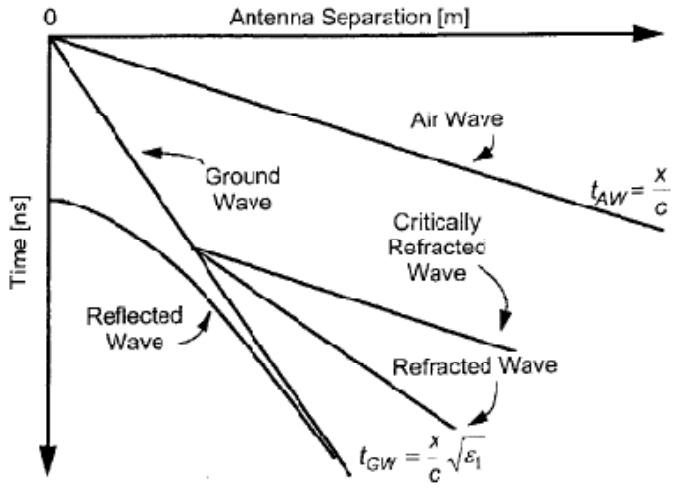

Fig. 22. Schematic wide angle reflection and refraction (WARR) measurement. (Huisman et al. 2001).

The relationship between ground wave arrival time (t_{GW}), antenna separation (x) and soil permittivity (e) is given by (Huisman et al. 2001) (Fig. 22).

$$\varepsilon = \left(\frac{c}{v}\right)^2 = \left[\frac{c(t_{GW} - t_{AW}) + x}{x}\right]^2 \tag{13}$$

4.1.5 Depth of penetration of GPR signals

Ground penetrating radar (GPR) with low antenna frequencies (25-200 MHz) can be used to detect moisture variation at depth less than 5m depending upon the mode in which waves are recorded. For example, if GPR is used to detect water content by recording ground waves then depth of penetration for these GPR signals would be 0-3m for (50MHz), and if it is used in reflection mode then it goes up to 24 m in depth.

The propagation velocity of radar waves (V) depends on the dielectric constant e of soil (Davis and Annan 1989):

$$V = \frac{V_{air}}{\sqrt{\varepsilon}} \tag{14}$$

The velocity in air (V_{air}) is 30cm ns^{-1}(Fig. 23). The dielectric constant of granular sediments is mainly governed by water content in that sediment, hence knowing the velocity of radar waves in ground we can evaluate the volumetric water content .

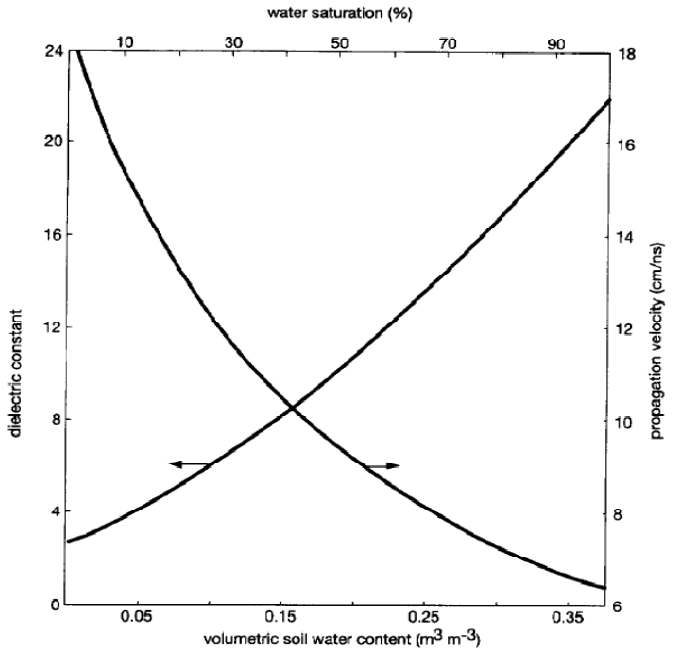

Fig. 23. The relation between soil water content and dielectric constant and propagation velocity of radar waves in unsaturated sands established with the Brugman-Hanai-Sen model (van Overmeeren et al. 1997).

Table 2. The influence of water on the propagation velocity of radar waves (van Overmeeren et al. 1997).

The influence of water on the propagation velocity of radar waves

Medium	Propagation velocity (cm ns^{-1})
Air	30
'Dry' sand	15
Water-saturated sand	6–7
Water	3.4

The ground waves travels directly from transmitter to receiver through the upper part of the ground. The velocity of ground waves depends on dielectric constant of the soil and hence on the soil water content and soil composition (Table 2.).

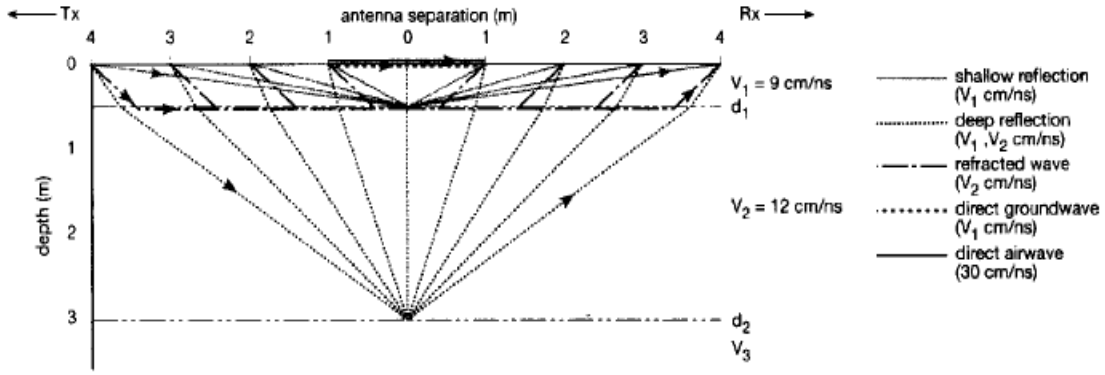

Fig. 24. Schematic wave paths of CMP (Common mid-point) measurements (van Overmeeren et al. 1997).

To detect boundaries for soil layers, a reflection coefficient of amplitude can be used (Fig. 24). The amplitude of waves is measured in terms of dielectric constant of materials at the boundary of different materials.

$$\rho = \left(\frac{\sqrt{\varepsilon_{r2}} - \sqrt{\varepsilon_{r1}}}{\sqrt{\varepsilon_{r2}} + \sqrt{\varepsilon_{r1}}} \right) \tag{15}$$

This equation gives more accurate results for detecting soil layers.

The depth of penetration depends upon the frequency of radar and the dielectric properties of material. The performance of radar signals is estimated by radar range equation. This equation is a function of system parameters and the electromagnetic properties of the material. The attenuation and velocity of radar signals are mainly governed by the soil condition(Morey 1998) (Fig. 25).

$$Q = 10\log\left(\frac{P_{\min}}{P_t} \right) = 10\log\left(\frac{E_t E_r G_t G_r v_m^2 g e^{-4\alpha R} \sigma}{64\pi^3 f^2 R^4} \right) \tag{16}$$

Q= System performance factor in decibels (dB)

e= base of natural logarithms.

System dependent parameters:

P_{min} = minimum detectable power,

P_t = transmitter output power to antenna,

E_t and E_r = antenna efficiency,

G_t and G_r = antenna gain,

and f = frequency of operation.

Media dependent parameters:

Vm = velocity of propagation in medium,

a=attenuation coefficient of medium,

Target dependent parameters:

g = hack scatter gain of target, and

S = target scattering cross-section area.

Range dependent parameters:

R = distance to target from antenna.

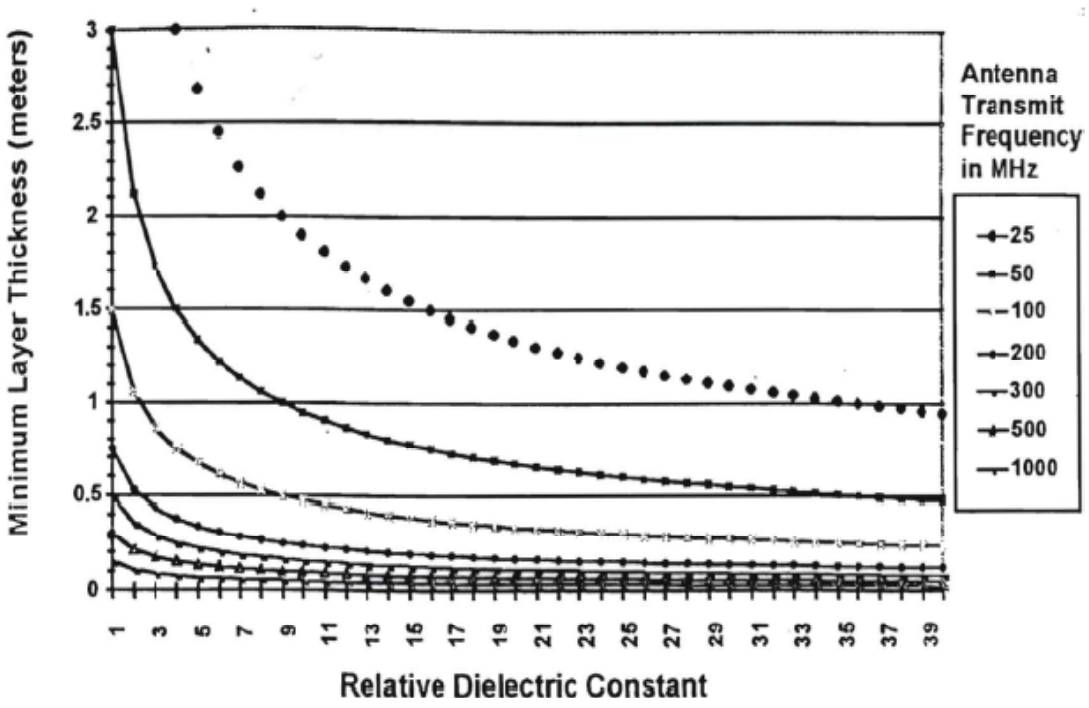

Fig. 25. Resolution as a function of operating frequency (Morey 1998).

4.2 Mathematical Mixing Models for the Determination of Dielectric Constant of Soils

There are various mathematical mixing models to predict dielectric properties of soils (geological materials); and each model has its own approach. These models are based on different approaches such as empirical models, phenomenological models, volumetric mixing formulas, effective medium theories, and semi-empirical model(Dobson et al. 1985).

The most widely used mixing models in the field of near-surface geophysical investigation are as follows:-

1. Empirical Models

   Polynomial Rule (Topp et al. 1980)

2. Volumetric mixing formulas

   Complex Refractive Index and Time Propagating models

   (Wharton et al. 1980).

3. Effective medium theories

   Bruggeman-Hanai-Sen Model (Sen 1981)

Apart from above mentioned models there are some semi-empirical models which are site specific and needs to be calibrated as per site conditions.

4.2.1 Empirical model

Polynomial Rule (Topp et al. 1980)

The empirical models are the simplest model for predicting dielectric properties of soils. These models are based on regression analysis on different minerals soils with clay content ranging from 9 to 66%. One of the simpler and most commonly used models is found by Topp et al (1980), is the third-order polynomial relationship between dielectric constant k(ε) and volumetric water content(θ_v).

$$\varepsilon = 3.03 + 9.30(\theta_v) + 146.00(\theta_v)^2 - 76.70(\theta_v)^3 \quad (17)$$

The error provided by the author stated that almost 93% of data fits in a band of $\pm 0.025\theta_v$. The above equation is inverted to find the volumetric content. The inverted form of this equation is mainly used by practioners of TDR (Time Domain Refelctometry) to find soil water content(Dasberg and Dalton 1985).

$$\theta_v = -5.3\times10^{-2} + 2.92\times10^{-2}(\varepsilon) - 5.5\times10^{-4}(\varepsilon)^2 + 4.3\times10^{-6}(\varepsilon)^3 \quad (18)$$

The main advantages of this model is that using dielectric properties of soil one can find volumetric water content without knowing any extra properties of soil. Disadvantages of this model are;1) This model is not demonstrated valid over the wide range of volumetric water content(VWC), clay contents and porosities(Roth et al. 1990).2) These equation are purely empirical.

4.2.2 Volumetric mixing models

Complex Refractive Index Model and Time Propagation Model(Wharton et al. 1980).

This model is based on volumetric relation of multiphase mixture. The dielectric constant of this multiphase mixture is related to dielectric constant and volumetric fraction of its individual constituents.

$$\varepsilon^{\alpha} = \sum_{i=1}^{N} V_i \varepsilon_i^{\alpha} \tag{19}$$

V_i and ε_i are the volume fraction and dielectric constant of ith component. The coefficient "α" in the above equation is geometrical factor. The α ranges from -1(series arrangement of dielectric components) to +1 (parallel arrangement of dielectric component). Equating α=0.5 in above volumetric equation gives the basic equation for CRIM & TP model(Knoll 1996).

$$\sqrt{\varepsilon} = \sum_{i=1}^{N} V_i \sqrt{\varepsilon}_i \tag{20}$$

In the above equation if a complex dielectric constant is used then it becomes equation for a Complex Refractive Index Model, and if a real part of dielectric constant is used then it forms an equation for Time Propagation Model.

Time Propagation (TP) Equation

$$\sqrt{\varepsilon} = \phi(1 - S_w)\sqrt{\varepsilon_a} + \phi S_w \sqrt{\varepsilon_w} + (1 - \phi) c l_v \sqrt{\varepsilon_{cl}} + (1 - \phi)(1 - c l_v)\sqrt{\varepsilon_s} \tag{21}$$

The TP equation is derived from the travel time calculations for electromagnetic waves through an isotropic material because; $\sqrt{\varepsilon}$ is proportional to the propagation time (Table 3. and 4.).

4.2.3 Effective medium theories

BHS Model (Bruggeman-Hanai-Sen Model) (Sen 1981)

The BHS Model is based on effective medium theories. These theories incorporate basic geometrical factors in their formula. The primary concept of these models is to determine material by successive substitutions. It starts with assuming homogenous background material, and then a small part of background material is replaced by another material. The most common and widely used model is BHS model, because of its accurate approximation for determining dielectric constant of saturated materials with non-interacting components(Sen 1981).

$$\phi = \left(\frac{\varepsilon_s - \varepsilon}{\varepsilon_s - \varepsilon_w} \right) \left(\frac{\varepsilon_w}{\varepsilon} \right)^d \tag{22}$$

where ε_s is dielectric constant of solids (grains), ε_w is dielectric constant for water, ε is dielectric constant of material, and d is the depolarization factor varies from 0 to 1 depending on the geometrical distribution and saturation of material(Knoll 1996). If the geometry of the solids is spherical then d=1/3.

Table 3. Dielectric constant value for different materials at 100 MHz frequency (Martinez and Byrnes 2001).

Material	ε_r (Davis and Annan,1989)	ε_r (Daniels,1996)
Air	1	1
Distilled water	80	-
Fresh water	80	81
Sea water	80	-
Fresh water ice	3-4	4
Sea water ice	-	4-8
Snow	-	8-12
Permafrost	-	4-8
Sand, dry	3-5	4-6
Sand, wet	20-30	10-30
Sandstone, dry	-	2-3
Sandstone, wet	-	5-10
Limestone	4-8	-
Limestone, dry	-	7
Limestone wet	-	8
Shales	5-15	-
Shale, wet	-	6-9
Silts	5-30	-
Clays	5-40	-

Table 3. continued

Material	ε_r (Davis and Annan,1989)	ε_r (Daniels,1996)
Clay, dry	-	2-6
Clay, wet	-	15-40
Soil, sandy dry	-	4-6
Soil, sandy wet	-	15-30
Soil, loamy dry	-	4-6
Soil, loamy wet	-	10-20
Soil, clayey dry	-	4-6
Soil, clayey wet	-	10-15
Coal, dry	-	3.5
Coal, wet	-	8
Granite	4-6	-
Granite, dry	-	5
Granite, wet	-	7

Table 4. Dielectric constant value for different materials at different frequency (Knoll 1996).

Material	**Dielectric Constant**	**Frequency (MHz)**	**Source**
Acetone	20.9	1	Lucius et al., 1989
Albite	7.0	1	Olhoeft, 1989
Air	1.0	1	Lucius et al., 1989

Table 4. continued

Material	Dielectric Constant	Frequency (MHz)	Source
Benzene	2.3	1	Lucius et al., 1989
Calcite	6.4	1	Olhoeft, 1989
Calcite	7.8–8.5	Radio	Keller, 1989
Carbon tetrachloride	2.2	1	Lucius et al., 1989
Chloroform	4.8	1	Lucius et al., 1989
Cyclohexane	2.0	1	Lucius et al., 1989
Ethylene glycol	38.7	1	Lucius et al., 1989
Gypsum	6.5	750	Martinez and Byrnes, 1999
Halite	5.9	1	Olhoeft, 1989
Ice	3.4	1	Olhoeft, 1989
Kaolinite	11.8	1	Olhoeft, 1989
Methanol	33.6	1	Lucius et al., 1989
Mica	6.4	750	Martinez and Byrnes, 1999
Montmorillonite	210	1	Olhoeft, 1989
Olivine	7.2	1	Olhoeft, 1989
Orthoclase	5.6	1	Olhoeft, 1989
Tetrachloroethene	2.3	1	Lucius et al., 1989
Trichloroethene	3.4	1	Lucius et al., 1989
Water	80	1	Lucius et al., 1989

4.3 Correlation between Dielectric Constant and Suction Using CRIM/TP Model

The dielectric constant can be evaluated using the above mentioned methods. But, the most widely used model is a Complex Refractive Index Model (CRIM) model, this model is extensively used in pavement monitoring and pavement quality control. The general form of equation is given is as follows.

$$\sqrt{\varepsilon_{mix}} = \sqrt{\varepsilon_s}\theta_s + \sqrt{\varepsilon_w}\theta_w + \sqrt{\varepsilon_a}\theta_a \tag{23}$$

where as

$$\theta_s = \frac{\gamma_d}{G_s\gamma_w} \tag{24}$$

$$\theta_w = \frac{w\gamma_d}{\gamma_w} \tag{25}$$

subsequently the equation for volumetric air content can be written as follows

$$\theta_a = 1 - \theta_w - \theta_s$$

substituting above volumetric content equations in an above CRIM model equation it gives out an equation which is stated below.

$$\sqrt{\varepsilon_{mix}} = \sqrt{\varepsilon_s}\left(\frac{\gamma_d}{G_s\gamma_w}\right) + \sqrt{\varepsilon_w}\theta_w + \sqrt{\varepsilon_a}\left(1 - \theta_w - \frac{\gamma_d}{G_s\gamma_w}\right) \tag{26}$$

rearranging above equation in terms of volumetric water content.

$$\theta_w = \frac{\sqrt{\varepsilon_{mix}} - \left(\frac{\sqrt{\varepsilon_s}\gamma_d}{G_s\gamma_w} + \sqrt{\varepsilon_a} - \frac{\sqrt{\varepsilon_a}\gamma_d}{G_s\gamma_w} \right)}{\left(\sqrt{\varepsilon_w} - \sqrt{\varepsilon_a} \right)} \tag{27}$$

Using above equation one can find the volumetric water content by knowing the dielectric constant of soil, dry density of soil, specific gravity of soil and dielectric constant of solid particles. But, the dielectric constant of solid particles is documented extensively for different types of soil constituents and the dielectric constant for water and air is 81 and 1 respectively.

The above calculated volumetric water content for a soil can be used to find the suction value for that soil by using Suction -Water content characteristic curve (SWCC)(Lytton et al. 2004). The equation for this curve is given as follows

$$S = -20.29 + 0.1555(LL) - 0.117(PI) + 0.0684(-\#200) \tag{28}$$

and for initial point on the curve is calculated using following equation

$$pF_0 = 5.622 + 0.0041(\%clay\ fines) \tag{29}$$

using this equation for the slope of this curve and initial point on the curve we can find suction value at any given volumetric water content by

$$pF(\theta_w) = pF_0 - \left|S\right| \frac{\gamma_w}{\gamma_d}(\theta_w) \tag{30}$$

Using these equations a program is written in Matlab® to find the suction for different dielectric constant values. Input parameters for this program are dielectric constant value of solids, range of dielectric constant value of soil, dry unit weight of soil, specific gravity, unit weight of water, liquid limit, plasticity index, percentage passing sieve #200 and percent amount of clay fines.

Using this program, different graphs were plotted with different input parameters. The following graphs are for pure Kaolinite with different dry density and rests of parameters were kept same. Similarly, a graph was plotted for a sample having 43% passing #200 sieve and 16% of fine clay particle with 1.732gm/cc as dry density. Most of the soils have dielectric constants ranging 20 to 40 and beyond 40 it gets too wet. Hence, the x-axis is limited to value from 20 to 40 (Fig. 26 to Fig. 28).

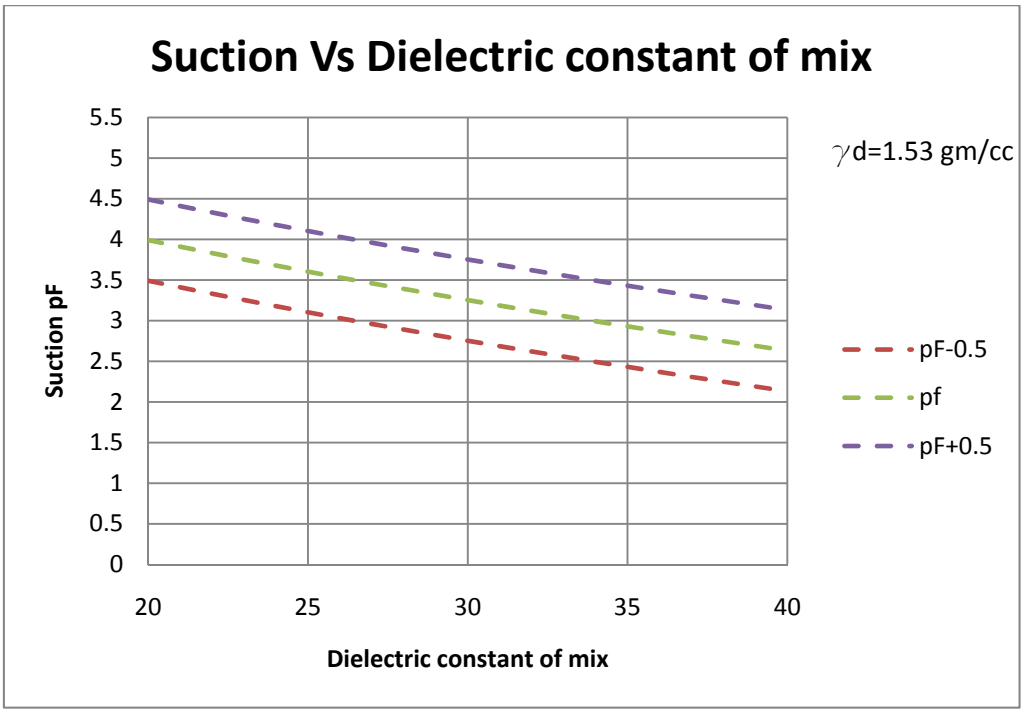

Fig.26. Theoretical correlation curve for pure kaolinite at dry density =1.53 gm/cc.

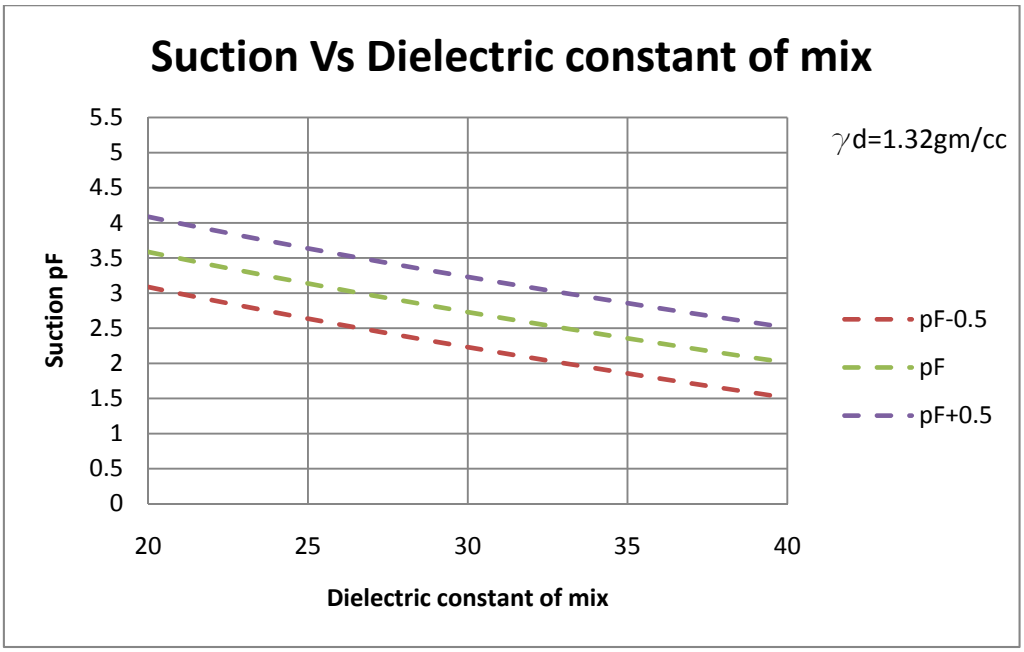

Fig.27. Theoretical correlation curve for pure kaolinite at dry density =1.32 gm/cc.

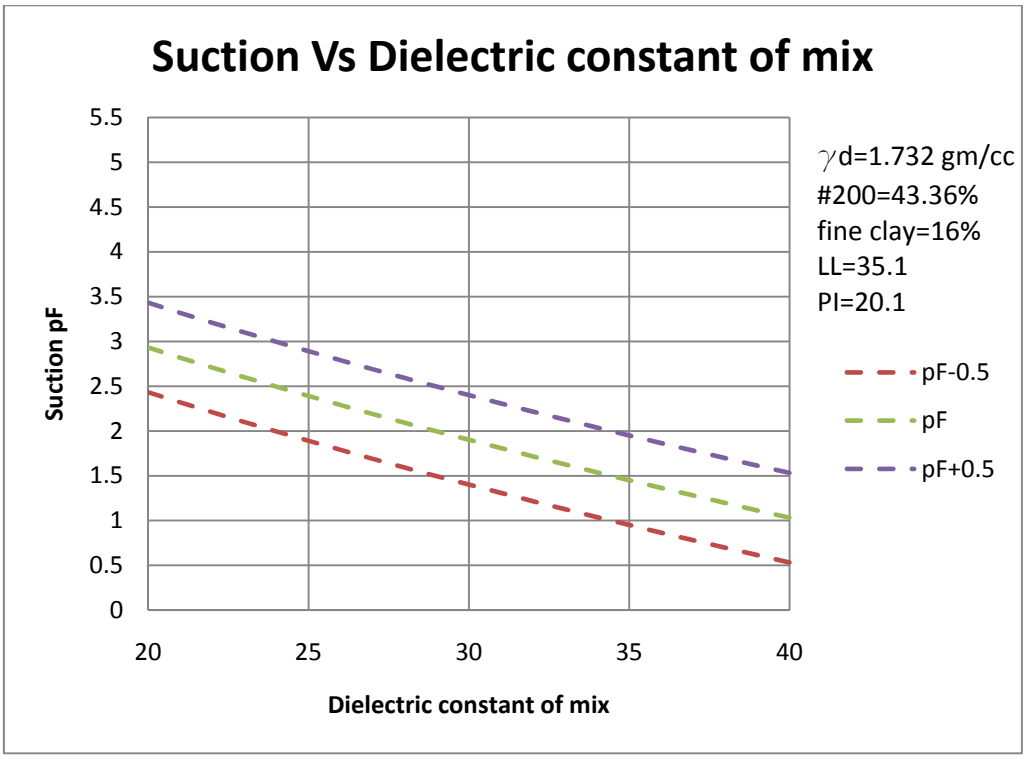

Fig. 28. Theoretical correlation curve for a normal soil at dry density =1.732 gm/cc.

To validate these graphs laboratory tests were conducted on these two samples. The first sample was pure kaolinite and other was a normal sample having 43% fines. Samples were made with different water contents ranging from w=24% to w=43% for clay and for clayey sand sample it was from w=11% to w=24%. After making these samples, a filter paper test was conducted to find the total suction for each specimen with a set of three points for same water content. And dielectric constants for these specimens were measured using percometer which works on similar principles of GPR. Detailed procedures for these tests are in written in appendix-C. Results from these tests

were compared with the theoretical study. Below shown figures (Fig. 29 and Fig. 30) are for pure clay sample.

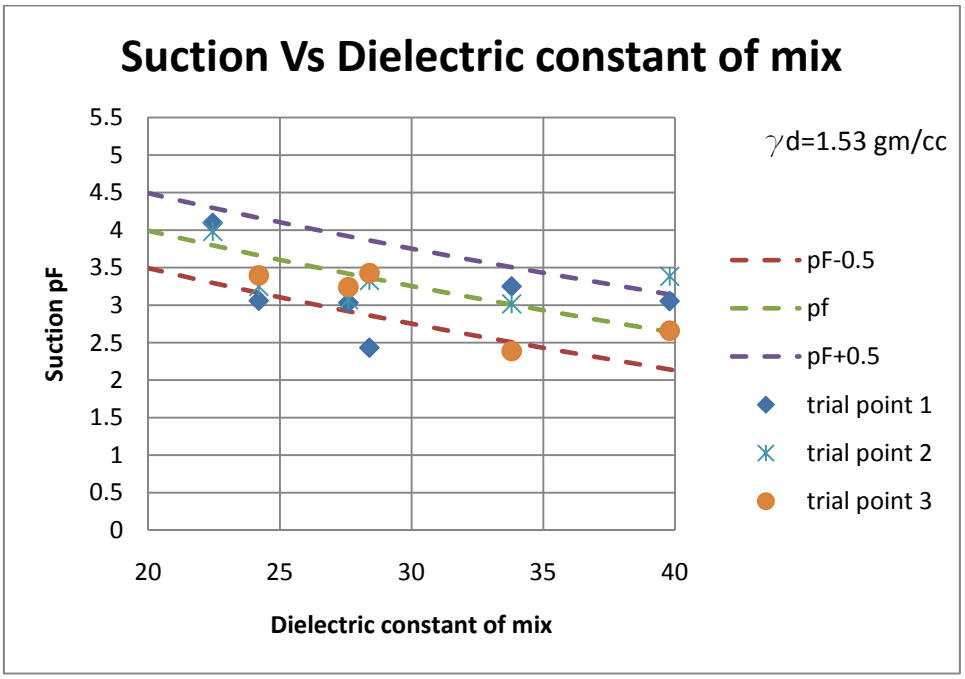

Fig. 29. Comparison of laboratory test data with theoretical curve at dry density =1.53 gm/cc.

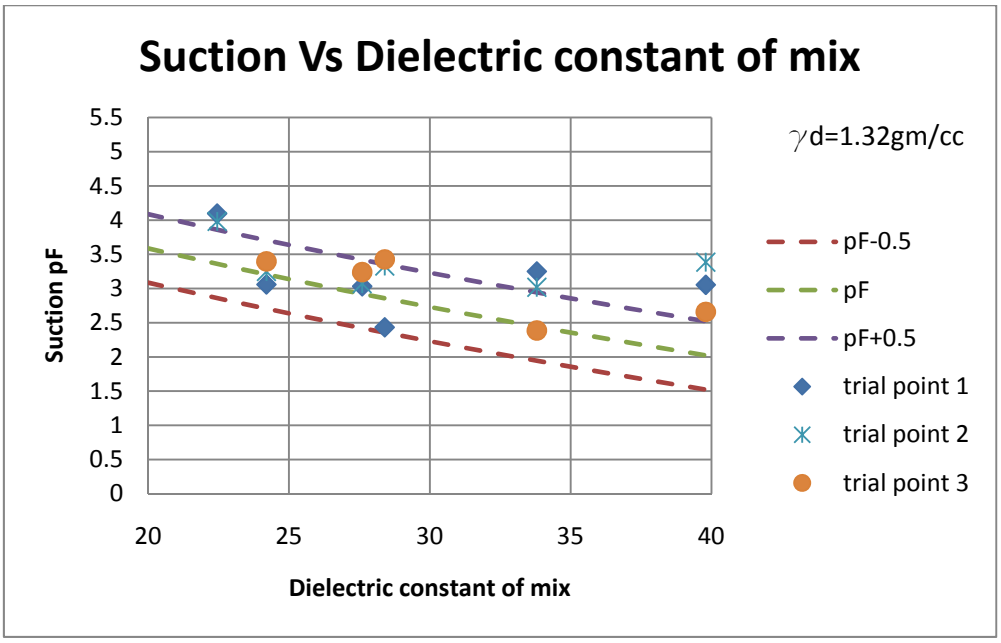

Fig. 30. Comparison of laboratory test data with theoretical curve at dry density =1.32 gm/cc.

A linear regression line is plotted for lab data to compare with theoretical curve, and the equation for that regression line is (Fig. 31):

$$y = -0.0741x + 5.2612 \quad (31)$$

$R^2=0.3922$

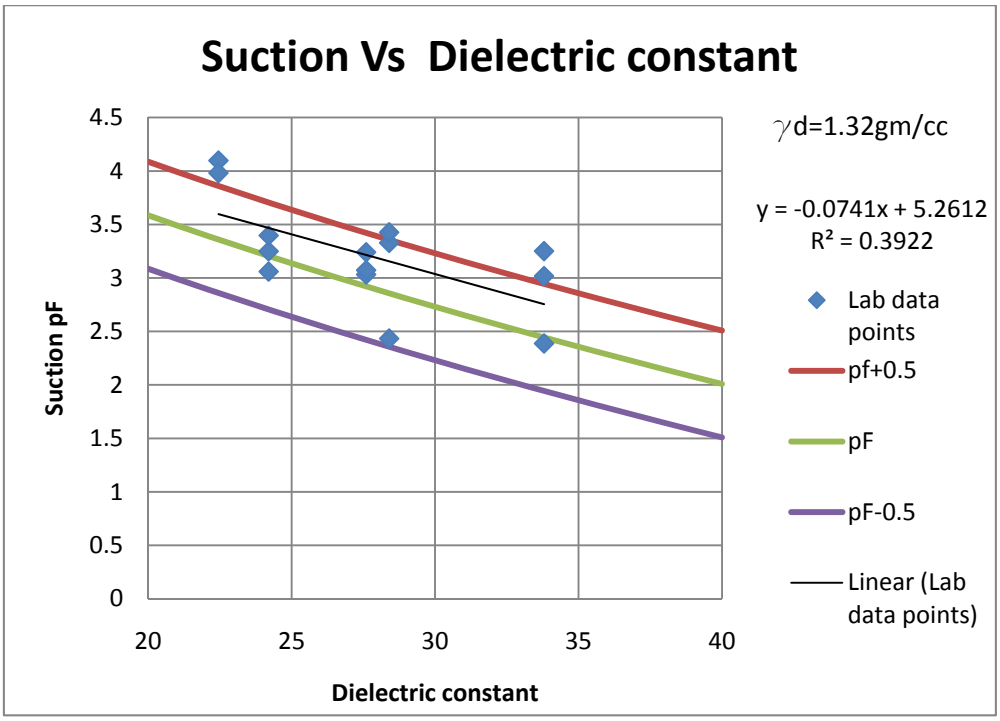

Fig. 31. Comparison of laboratory test data points and linear regression line with theoretical curve at dry density =1.32 gm/cc.

The filter paper results for a normal soil were compared with the theoretical study to make a correlation and to validate the study. The graph shown below is for a normal soil.

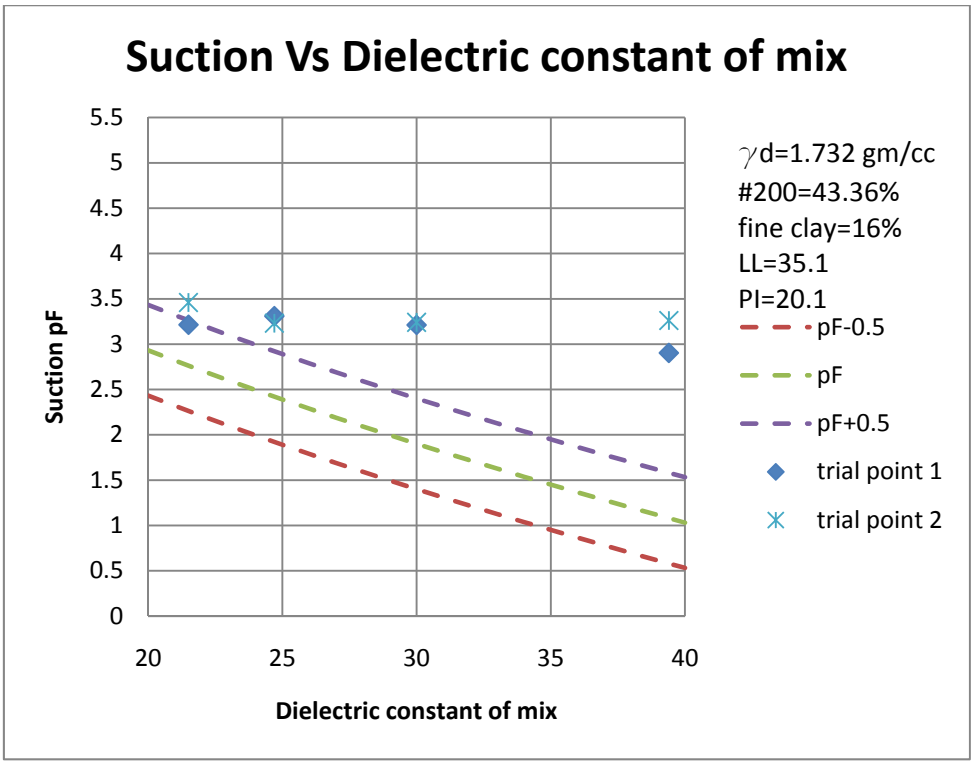

Fig. 32. Comparison of laboratory test data points with theoretical curve for a normal soil sample at dry density =1.732gm/cc.

In above graphs dashed lines are theoretical curve generated from correlation and points are the laboratory data points. The laboratory data for this soil sample shows that the suction is in a range of 3.5pF to 2.6 pF because the calibration curve for filter paper test holds good to the point where suction value is 2.5pF. Therefore, this sample will need more data points on drier side of suction scale to make a good correlation with theoretical study. The calibration curve for filter paper test is shown in Appendix-(C). This sample was more sandy and for most of the sandy soils the suction value changes drastically (Fig. 32), the slope of suction-water content curve for this soil was steeper as

compared to clayey soil and the filter paper test can give reasonable values till 2.5 pF due the calibration curve for filter paper test.

4.4 Improvements in Technology for Geotechnical Purposes

GPR (Ground penetrating radar) has been used in different fields such as in geology to locate the sinkholes and to find rock fissures. It is also used in sedimentology to assess the sediment process and to identify the different type of sedimentary structure (Neal 2004). The GPR is also used in transportation field as a Non-destructive testing instrument. In the field of pavements, GPR is used for a pavement evaluation to make a decision for optimal maintenance, to measure the thickness of layer, to detect the subsurface defects and it is also used as non-destructive instrument to find the type of soil of a subgrade (Saarenketo and Scullion 2000). The advantage of GPR as Non destructive instrument for soil profiling is that it gives a continuous data across the test length. Apart from the usage of GPR in Pavements, it is also used extensively in railway industry for track maintenance, ballast composition, type of ballast and check for good drainage along the track. (Olhoeft et al. 2002)

Dielectric constant is a constituent property of any given material. Water has a dielectric constant value as 81. Soil is considered as mix of three different materials such as soil solids, water and air. The amount of these material present in a soil governs the dielectric property of a given soil mix. As GPR measures the dielectric constant for a given material, it has been used for measuring soil moisture, frost susceptibility of soils

(Saarenketo and Scullion 2000). GPR is also used in railways to detect the moisture pockets in ballast (Olhoeft et al. 2002).

The shear strength of soil depends on its moisture content. As moisture content increases shear strength of a soil decreases leading to the loss of its capacity. Suction value for a soil is also dependent upon the water content. Suction value has its importance in defining shear strength in unsaturated soils as, suction value increases shear strength also increases. Therefore, it is very important to know the suction value of a soil to estimate the shear strength.

GPR is used to determine the dielectric constant of a given material. GPR is significant in soil mechanics due to the correlation between the dielectric constant of a given soil and its moisture content. Also, it has been stated in this research study that the suction value of soils is influenced by changes in water content, which in turn, can be related to the dielectric constant of the soil.

In this research study, a correlation has been made between suction and dielectric constant to quantify the use of GPR as an instrument to the estimate suction value. The study showed that GPR can play an important role in estimating suction value of railway embankments by measuring dielectric constant value. This suction value can be used to predict the strength of these embankments. Currently, GPR gives the tomography of variation of dielectric constant value along the test profile and this data has to be interpreted in terms of type of soil and water content and predicting the suction value for respective soil type by using above established correlation between suction value and

dielectric constant value. To do the interpretation of dielectric value for predicting suction, a parametric study is carried out to explain how use this correlation and this study explains how to generate correlation curves and using them.

A parametric study has been conducted using the correlation between suction value and dielectric constant, and data for this equation were taken from web soil survey(National Resources Conservation Service 2009). This study was conducted by taking data from the soil survey website for surface soils along the railroad line from Wellborn Texas to Bryan, Texas. Using engineering properties for surface soils along this stretch, a correlation graph is plotted for different type soils. The depth for these surface soils in this website was considered to the depth of 14 inch. There was large variation in soil property along the depth; therefore only surface soil was considered for this initial parametric study. The types of soils and their properties along the stretch of this railroad are tabulated below (Table 5.). Specific gravity for these soils is assumed as 2.72 and it is found out that the result does not change with a change in specific gravity, as the range for specific gravity for most of soils are from 2.65 to 2.72.

Table 5. Engineering properties of surface soils along the rail track from Wellborn-Texas to Bryan-Texas from websoil survey website(National Resources Conservation Service 2009).

Sr No	Soil Type	Depth (in)	Classification	Gs	γt at 1/3 of a bar (gm/cc)	θ_w at 1/3 of a bar	#200	%fine clay	LL	PI
1	MaA—Mabank loam, 0 to 1 percent slopes	0-8	SC, SC-SM, CL, CL-ML	2.72	1.58	28.1	40-70	17.5	19-32	4-15
2	TaA—Tabor fine sandy loam, 0 to 2 percent slopes	0-14	ML, SC-SM, SM, CL-ML	2.72	1.38	18.8	30-55	14	15-25	NP-7
3	LfA—Lufkin fine sandy loam, 0 to 1 percent slopes	0-9	CL, ML, SC, SM	2.72	1.5	17.7	40-85	11.5	15-30	NP-10
4	BwC—Burlewash fine sandy loam, 1	0-8	ML, SC-SM, SM, CL-ML	2.72	1.38	17.1	40-60	10	0-25	NP-7

Table 5. continued

Sr No	Soil Type	Depth (in)	Classification	Gs	γt at 1/3 of a bar (gm/cc)	θ_w at 1/3 of a bar	#200	%fine clay	LL	PI
5	Sa—Sandow loam, frequently flooded	0-6	SC-SM, CL, CL-ML, SC	2.72	1.3	28.6	45-60	20	25-40	6-20
Sr No	Soil Type	Depth (in)	Classification	Gs	γt at 1/3 of a bar (gm/cc)	θ_w at 1/3 of a bar	#200	%fine clay	LL	PI
6	GrC—Gredge fine sandy loam, 1 to 5 percent slopes	0-7	SM, CL-ML, ML, SC-SM	2.72	1.43	17.2	35-55	11	0-31	NP-7
7	ZuB—Zulch fine sandy loam, 1 to 3 percent slopes	0-5	SC-SM, SM, CL-ML, ML	2.72	1.6	17.2	40-60	8	15-30	NP-7

Table 5. continued

Sr No	Soil Type	Depth (in)	Classification	Gs	γt at 1/3 of a bar (gm/cc)	θ_w at 1/3 of a bar	#200	%fine clay	LL	PI
8	DeA—Derly-Rader complex, 0 to 1 percent slopes	0-6	CL, CL-ML, ML	2.72	1.5	25.9	55-90	14	0-30	NP-10
9	BrB—Boonville-Urban land complex, 0 to 3 percent slopes	0-12	ML, SC-SM, SM, CL-ML	2.72	1.42	16.2	40-65	10	0-20	NP-7
10	BoB—Boonville fine sandy loam, 1 to 3 percent slope	0-17	CL-ML, ML, SC-SM, SM	2.72	1.42	16.2	40-65	10	0-20	NP-7
11	Sb—Sandow-Urban land complex	0-6	CL, CL-ML, SC, SC-SM	2.72	1.3	28.6	45-80	20	25-40	6-20

Table 5. continued

Sr No	Soil Type	Depth (in)	Classification	Gs	γt at 1/3 of a bar (gm/cc)	θ_w at 1/3 of a bar	#200	%fine clay	LL	PI
12	BoA—Boonville fine sandy loam, 0 to 1	0-17	ML, SC-SM, SM, CL-ML	2.72	1.42	16.2	40-65	10	0-20	NP-7
13	Ur-Urban land	0-40	-	-	-		-	-	-	-
14	ZcB—Zack-Urban land complex, 1 to 5 percent slopes	0-7	ML, SM	2.72	1.23	16.1	40-65	11	20-30	NP-7

Using above data for different type of soils, total suction was predicted for these soils by using correlation equation between suction and dielectric constant which has been explained above in this section (Fig. 33).

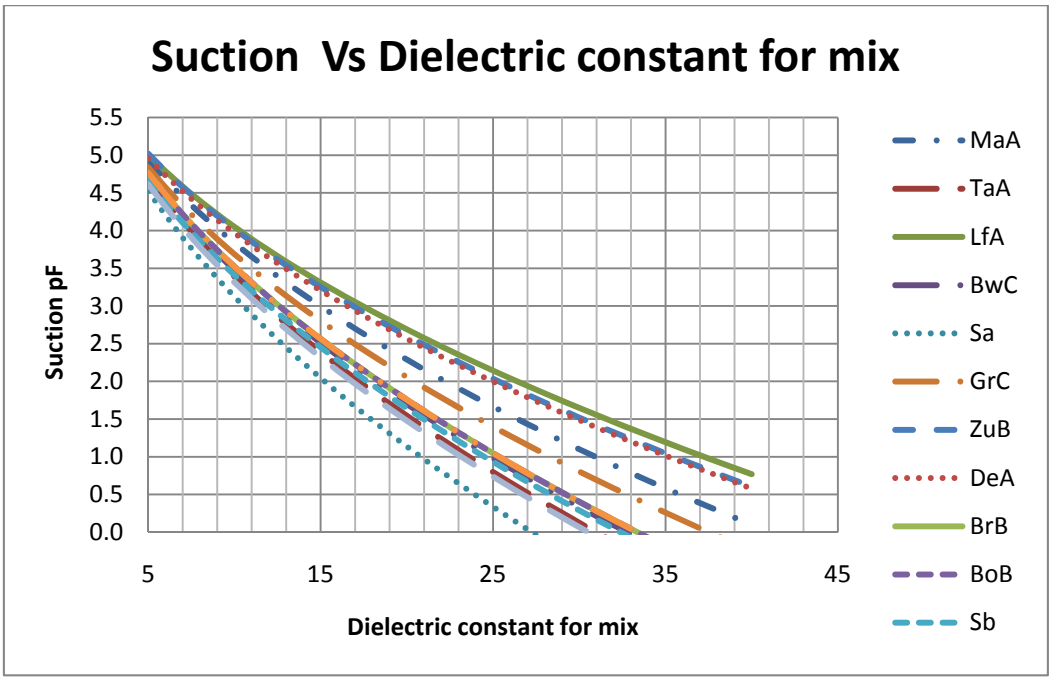

Fig. 33. Theorectical correlation curve for surface soils along the rail track from Wellborn-Texas to Bryan –Texas.

In this parametric study a corelation curves were generated from the least possible value of dielectric constant for any given soil to the highest value (almost wet soil). From correlation cuvres it shows that the suction value is dependent on percent fine clays ,Liquid limit and plasticity index which are the basic test performed in laborotary or this data can be obtained from websoil survey data for any given area for surface soils as well as for deep soils upto 6 ft deep. To generate these cruves a program is written in Matlab® which is explained in appendix-A-3.

5. CONCLUSION

5.1. Summary

In this research study, a literature rewiew on current pratices in wireless monitoring of slopes was carried out. This review has mainly covered two types of monitoring systems, one which uses rainfall intensity data to trigger the warning system. In other type of system , an Inclinometer and soil moisture sensor were used to record the movement and change in water content for that slope. In the rainfall intesity type monitoring, rain gauges were installed and using the empirical formula for intensity calcualtion an early warning system was established along the coast of Edmonds Washington(Baum et al. 2005). This type of system is beneficial if there are proper geological data for that site and a good understanding about the erosion process for different geological deposits. The other type of monitoring system is installed on engineered slopes to monitor the movement of slope during the rainfall season. In this system, an Inclinometer and moisture sensor are used to measure the movement and water content respectively and this data was stored onsite on a data logger. The data from a data logger was transmitted wirlessly to the monitoring station.

Based upon litreature reiveiw, an assesement of commerically available instruments was done. The assessment of instruments were based on following criteria:

- Low Cost

- Low maintenance
- Expandable for future technology
- Work efficiently during extreme weather conditions
- Low power consumption

The MEMS accelerometer used as tiltmeter fulfills most of the above criteria. Therefore, it is a promising tool for monitoring railway embankments.

Prior to the deployment of the monitoring system, a suction-moisture infiltration model should be developed to study the effects of crack depth, moisture diffusion, and the angle of the slope. Using this model, the factor of safety of the slope at various depths can be evaluated. This model provides useful information for the deployment of instruments along the depth of slope to minimize the number of instruments installed for that slope.

In this research another approach, GPR, for monitoring these railway embankments was investigated. The study evaluated the potential for using GPR as a tool for evaluating moisture variation on railway embankments. The working principle and a background of GPR were discussed in this thesis. GPR measures the variation in dielectric constant which is depends on material constituents and volumetric content of different materials in a mixture. Each material has different dielectric constant value and water has the highest value. The change in dielectric value for a soil (mixture) determines the volumetric water content in that soil. To know the exact amount of

different materials in a mixture, different mixing models for soils were explained and evaluated. The most widely used model to evaluate the volumetric content was the CRIM/TP model. This model uses volumetric content of individual constituents in a mix to calculate the dielectric constant of the mix. Using this model, the water content of a given soil may be back-calculated. In addition, a correlation between suction value and dielectric constant was established. The suction value for any given soil depends on amounts of fines, amount of clay fines, liquid limit, plasticity index and volumetric water content. The suction water content curve was used to explain the effect of water content on suction value for any given soils.

Since the dielectric constant for a soil is a function of water content, and suction is a function of water content, soil suction can be directly estimated from the measured dielectric constant of a soil. To validate this approach, a laboratory study was conducted on pure kaolinite and a soil sample with 16% clay fines. Filter paper tests were performed on these samples to measure suction. The dielectric constants of the same samples were measured using a percometer. For pure kaolinite, the laboratory data agreed well with the theoretical correlation curve. However, suction values as low as 2.5pF were measured on the soil sample with 16% clay fines, which is the lower limit on calibration curve of filter paper test. Therefore, it was difficult to draw definitive conclusions from the study of this sample.

5.2. Conclusion

It would be very expensive to install wireless instrumentation on all railway embankments to monitor the stability. Therefore, a preliminary site assessment should be done to identify failure prone areas. This assessment would reduce the number of instruments to be deployed in a monitoring system and it will also reduce the redundancies in monitoring system. The instrumentation of railway embankments works effectively and inexpensively when the target area for monitoring is limited in spatial extent. Thus, wireless monitoring can be considered as an effective tool for monitoring specific locations that have been identified to be prone to failure. Therefore, wireless monitoring should be considered in conjunction with a larger monitoring program that involves preliminary identification of failure prone areas which will more intensive monitoring. The later part of this research study dealt with the potential use of GPR as an assessment and a monitoring device for these railway embankments. In this research study, a background about a use of GPR in different field was explained. And different types of soil mixing models were discussed to find out the amount of individual constituent was present in a soil mix. The most common mixing model for soils was used to evaluate the volumetric contents of different material. The model is known as CRIM/TP model which is widely used to find the volumetric water content of a soil based upon the dielectric constant value of that soil. This model was used to formulate the correlation between suction and dielectric constant as both were dependent on volumetric water content of a soil. The suction value also depends on percent amount of passing # 200 sieve, percent amount of fine clays, liquid limit and plasticity index of a given soil. Using this correlation, curves were generated for pure kaolinite and for a

normal soil having 42% passing #200 sieve fines. These curves were validated by performing filter paper test to find suction and using percometer to determine the dielectric constant value at different volumetric water content. From above laboratory study, the experimental data for clay follows the trend of theoretical curve. This correlation can be used to predict the suction value based upon the dielectric constant value for a given soil. This suction values helps in estimating the stability of slopes, in compacted high plastic clays slopes if a suction value goes below 2 pF then there is a high change of shallow slope failure (Aubeny and Lytton 2004). To generate the correlation curves for railway embankments, a good database on soils used to construct them is required. This database should contain engineering properties of soils. Otherwise, these engineering properties of soil can be retrieved from websoil survey website which gives data for all soils mapped in this website. This type of monitoring system needs more research and field study to validate the correlation curve. Therefore, this type of monitoring system can be used as an assessment tool for deploying long-term monitoring systems.

5.3. Proposed Plan for Future Research

This research study has shown the potential use of wireless instruments and GPR as a monitoring device in geotechnical field to monitor slope stability. This research has mainly targeted applications for railway embankment monitoring against shallow slope failure. More field study should be carried out for these wireless instruments to develop a robust monitoring system. This field evaluation can be done at National Geotechnical

Experimentation Site at Texas A&M university Riverside campus. In this field evaluation these instruments should be calibrated for field conditions and then a reliability study should be carried out by comparing the data with the traditional In-Place Inclinometers. This study will address the issue of false positives for monitoring systems. After field evaluation of these instruments, a trial monitoring system can be installed along the railway embankment in Bryan/College Station area.

The use of GPR as a monitoring device can be assisted by more field study on different soils. The field study for GPR should include the classification and evaluation of engineering properties of soils in the test program, and this study should validate the correlation between suction and dielectric constant based on field measurements. After refining the correlation curve from field studies, GPR should be used to measure the dielectric constant and then estimate the suction value for a given soil. Suction values inferred from GPR data should be cross-checked through independent comparisons to other suction measurement methods.

REFERENCES

Aubeny, C., and Lytton, R. (2004). "Shallow slides in compacted high plasticity clay slopes." *Journal of Geotechnical and Geoenvironmental Engineering*, 130(7), 717-727.

Baum, R., Godt, J., Harp, E., McKenna, J., and McMullen, S. (2005). "Early warning of landslides for rail traffic between Seattle and Everett, Washington, USA." *Landslide Risk Management*, 731-740.

Baum, R., Harp, E., Hultman, W., and Survey, G. (2000). *Map showing recent and historic landslide activity on coastal bluffs of Puget Sound between Shilshole Bay and Everett, Washington*, U.S. Geological Survey. http://pubs.usgs.gov/mf/2000/mf-2346/mf-2346so.pdf.(June 17,2008)

Bulut, R., Lytton, R., and Wray, W. (2001). "Soil suction measurements by filter paper." *ASCE Geotechnical Special Publication*, 243-261.

Caine, N. (1980). "The rainfall intensity: duration control of shallow landslides and debris flows." *Geografiska Annaler. Series A. Physical Geography*, 23-27.

Campbell Scientific, I. (2008). Online Quote for instruments .http://www.campbellsci.com/. (June 17,2008)

Chen, H., and Lee, C. (2003). "A dynamic model for rainfall-induced landslides on natural slopes." *Geomorphology*, 51(4), 269-288.

Crossbow Technology, I. (2008). "Product reference guide". http://www.xbow.com/Support/Support_pdf_files/Product_Feature_Reference_Chart.pdf. (May 5,2008)

Dasberg, S., and Dalton, F. (1985). "Time domain reflectometry field measurements of soil water content and electrical conductivity." *Soil Science Society of America Journal*, 49(2), 293.

Davis, J., and Annan, A. (1989). "Ground-penetrating radar for high-resolution mapping of soil and rock stratigraphy 1." *Geophysical Prospecting*, 37(5), 531-551.

Decagon Devices, I. (2008a). "EC-20, EC-10,EC-5 Soil moisture sensors user's manual". http://www.decagon.com/pdfs/manuals/EC-20_EC-10_EC-5_v8.pdf. (May 5,2008)

Decagon Devices, I. (2008b). "Tensiometers", http://www.decagon.com/.(May 5,2008)

Dobson, M., Ulaby, F., Hallikainen, M., and El-Rayes, M. (1985). "Microwave dielectric behavior of wet soil-Part II: Dielectric mixing models." *IEEE Transactions on Geoscience and Remote Sensing*, 35-46.

Dowding, C., and O Connor, K. (2000). "Comparison of TDR and Inclinometers for slope monitoring." *ASCE geotechnical special publication No 106*, ASCE,Reston,VA.80-90.

Fredlund, D., and Rahardjo, H. (1993). " *Soil mechanics for unsaturated soils*." John Wiley and Sons. New York:

Furlani, K., Miller, P., and Mooney, M.,(2005), "Evaluation of Wireless Sensor Node for Measuring Slope Inclination in Geotechnical Applications." *Proceeding of the 22nd International Symposium on Automation and Robotics in Construction*,Ferrara,Italy,11–14.

Garich, E. (2007). "Wireless, automated monitoring for potential landslide hazards," M.S-Thesis.Texas A&M University,College Station,TX.

Hoekstra, P., and Delaney, A. (1974). "Dielectric properties of soils at UHF and microwave frequencies." *J. Geophys. Res*, 79(11), 1699–1708.

Hoffman, K., Varuso, R., and Fratta, D.(2006) "The use of low-cost MEMS accelerometers for the near-surface monitoring of geotechnical engineering systems.". *ASCE Conf. Proc. 187, GeoCongress 2006 Conference,*ASCE, Atlanta, GA,38-43

Holtz, R., and Kovacs, W. (1981). *An introduction to geotechnical engineering*, Prentice Hall, Englewood Cliffs, NJ.

Huisman, J., Sperl, C., Bouten, W., and Verstraten, J. (2001). "Soil water content measurements at different scales: accuracy of time domain reflectometry and ground-penetrating radar." *Journal of Hydrology*, 245(1-4), 48-58.

Huisman, J. A., Hubbard, S. S., Redman, J. D., and Annan, A. P. (2003). "Measuring soil water content with ground penetrating radar a review." *Vadose Zone Journal*, 2(4), 476-491.

Hungr, O. (2005). *Landslide risk management*, Taylor & Francis, London, pp. 99–128..

Kane, W., and Beck, T. (2000). "Instrumentation practice for slope monitoring." *Engineering Geology Practice in Northern California.* Association of Engineering Geologists, Sacramento and San Francisco Sections, CA.

Kane, W., Beck, T., and Hughes, J(2001). "Applications of time domain reflectometry to landslide and slope monitoring." *Proceedings of the Second International Symposium and Workshop on TDR*, Evanston, Illinois 305-314.

Knoll, M. (1996). "A petrophysical basis for ground penetrating radar and very early time electromagnetics: electrical properties of sand-clay mixtures". PhD Thesis, University of British Columbia, Vancouver, Canada.

Lynch, J., and Loh, K. (2006). "A summary review of wireless sensors and sensor networks for structural health monitoring." *Shock and Vibration Digest*, 38(2), 91-130.

Lytton, R., Aubeny, C., and Bulut, R. (2004). "Design procedure for pavements on expansive soils." *Research Report FHWA/TX-05/0-4518-1*, Texas Transportation Institute, Texas A&M University, College Station, TX.

Martinez, A., and Byrnes, A. (2001). "Modeling dielectric-constant values of geologic materials: An aid to ground-penetrating radar data collection and interpretation." *Current Research in Earth Sciences, Bulletin*, 247, 1–16.

Minard, J., and Survey, G. (1983). Geologic map of the Edmonds east and part of the Edmonds west quadrangles, Washington,WA, *US Geological Survey Miscellaneous Field Studies Map MF–1541.*

Morey, R. (1998). "Ground penetrating radar for evaluating subsurface conditions for transportation facilities", *NCHRP Synthesis of Highway Practice 255,* TransportationResearch Board, National Research Council, Washington, DC

National Resources Conservation Service, (2009)."Websoil Survey Website" U. S. Department of Agriculture, Washington, DC 20250.

Neal, A. (2004). "Ground-penetrating radar and its use in sedimentology: principles, problems and progress." *Earth Science Reviews*, 66(3-4), 261-330.

Olhoeft, G., Selig, E., and Inc, E.(2002) "Ground penetrating radar evaluation of railway track substructure conditions." *Proceedings of 9th International Conference on Ground Penetrating Radar,* Santa Barbara, CA, 48-53.

Roth, K., Schulin, R., Fluhler, H., and Attinger, W. (1990). "Calibration of time domain reflectometry for water content measurement using a composite dielectric approach." *Water Resour. Res*, 26(10), 2267-2273.

Saarenketo, T., and Scullion, T. (2000). "Road evaluation with ground penetrating radar." *Journal of Applied Geophysics*, 43(2-4), 119-138.

Sen, P. (1981). "Relation of certain geometrical features to the dielectric anomaly of rocks." *Geophysics*, 46, 1714.

Slope Indicator, L. (2006). "EL In-Place inclinometer datasheet." http://www.slopeindicator.com/instruments/inclin-intro.html.(May 5,2008)

Spiker, E., and Gori, P. (2003). "National landslide hazards mitigation strategy-A framework for loss reduction (Circular 1244)." *US Geological Survey,* Reston, VA, http://pubs. usgs. gov/circ/c1244/c1244. pdf.

Topp, G., Davis, J., and Annan, A. (1980). "Electromagnetic determination of soil water content: measurements in coaxial transmission lines." *Water Resources Research*, 16(3) 574–582.

van Overmeeren, R., Sariowan, S., and Gehrels, J. (1997). "Ground penetrating radar for determining volumetric soil water content; results of comparative measurements at two test sites." *Journal of Hydrology*, 197(1-4), 316-338.

Wharton, R., Hazen, G., Rau, R., and Best, D. (1980). "Electromagnetic propagation logging: Advances in technique and interpretation." *SPE 55th Annual Technical Conference and Exhibition,*Dallas,TX,Paper,9267. 1-12.

APPENDIX A-1

In this section, a MATLAB® program for moisture infiltration and crack depth to find the factor of safety along the depth is explained. The input parameters for this program are as follows:

1. Coefficient of moisture diffusion
2. Depth of slope
3. Number of increments along the depth
4. Dry suction value
5. Wet suction value
6. Angle of slope
7. Unit weight of soil and water
8. Angle of internal friction
9. Cohesion
10. Depth of cracks

The Matlab® program code is given below

```
% program to analyze moisture active zone moisture suction envelope
% for 2-step surface suction function
% programmed by charles p. aubeny, February 2006
% edited for Factor of safety calcualtion by vishal Dantal, August 2009
clear all
```

```
% input data Case1
alpha=4.18;%input('enter alpha in m2/yr   ');
ymax=input('enter ymax in meters  ');
ny=input('enter number of y increments   ');
n=1;%input('enter frequency of climatic cycles in years   ');
udry=input('enter dry suction   ');
uwe=input('enter wet suction   ');
ue=input('enter equilibrium suction   ');
A=input('enter angle of slope in degree   ');
TW= input('enter total unit weight of soil in kN/m3    ');
gw= 10;%input('enter unit weight of water in kN/m3    ');
PHI=input('enter angle of internal friction in degree   ');
cho=input('enter cohesion of soil in kpa    ');
osm= 2;%input('enter osmotic suction in pF  ');
dc=input('enter the depth of cracking in meters    ');
af=1.4;
dudry=udry-ue;
u0=udry-uwe;
phi=dudry/u0;

Ar=(A*pi/180);
PH=PHI*pi/180;

% convert to consistent units (meters and years)
%alpha=alpha*3154/3154;

nterm=100;
```

```
y=linspace(0,ymax,ny);
y1=y*cos(Ar);
%compute fourier coefficiencts
for k=1:nterm
   a(k)=(2/(pi*k))*sin(k*pi*(1-phi));
end



%x=1;
%f=0;
%for k=1:nterm
%    f=f+a(k)*cos(k*x);
%end
%answer=f

%compute suction envelope
 duwet(1:ny)=0;
A(1:ny)=0;
for l=1:ny
 if y1(l)<=dc;
    A(l)=0;

 else
    A(l)=y1(l)-dc;
 end
end
```

```
lambda1=pi*(A).^2*n/alpha;
lambda=pi*(y1).^2*n/alpha;
dudry(1:ny)=0;

for k=1:nterm

   phased=  (lambda).^0.5*k-(lambda*k).^0.5;
   phasew=(pi+(lambda1).^0.5)*k-(lambda1*k).^0.5;
   dudry=dudry+a(k)*u0*exp(-(k*lambda).^0.5).*cos(phased);
    duwet=duwet-a(k)*u0*exp(-(k*lambda1).^0.5).*cos(phasew);
end

udry(1:ny)=0;
udry=dudry+ue;
uwet=ue-duwet;


%find moisture active zone depth
duma=0.1*(dudry(1)-duwet(ny));
for i=1:ny
   if dudry(i)-duwet(ny-i)<duma
      deltadry=dudry(i)-dudry(i-1);
      deltawet=duwet(ny-i)-duwet((ny-i)-1);
      deltau=deltadry-deltawet;
      deltay=y1(i-1)-y1(i);
      slope=deltay/deltau;
      deltau=duma-dudry(i)+duwet(ny-i);
```

```
        yma=y1(i)-deltau*slope;
        break
    end
end
%calculation of factor of safety for slope
for j=1:ny

UW(j)=-(10^uwet(j))/100;

fUW(j)=UW(j)-(-(10^osm)/100);
Y(j)=(fUW(j)+y1(j))*cos(Ar);
poresh(j)=(sqrt(2/3)*af*TW*y1(j)*sin(Ar)*cos(Ar));
porest(j)=gw.*(Y(j));
poret(j)=porest(j)+poresh(j);
T(j)=(cho+(TW*y1(j)*(cos(Ar))^2-poret(j))*tan(PH));
D(j)=(TW*y1(j)*sin(Ar)*cos(Ar));
FS(j)=T(j)/D(j);

end

%results
    udry1=transpose(udry);
    uwet1=transpose(uwet);
    y3=transpose(y);
    y4=transpose(y1);
    FS1=transpose(FS);
    plot(udry,(y),uwet,(y));
```

```
 set(gca,'Ydir','reverse');
 xlabel('Suction in pF');
 ylabel('depth in M');
legend('dry suction','wet suction');
grid on

Figure (2)
Plot ((y), FS);
ylabel('FS');
 xlabel('depth in M');
 grid on
```

Output of this program is as follows

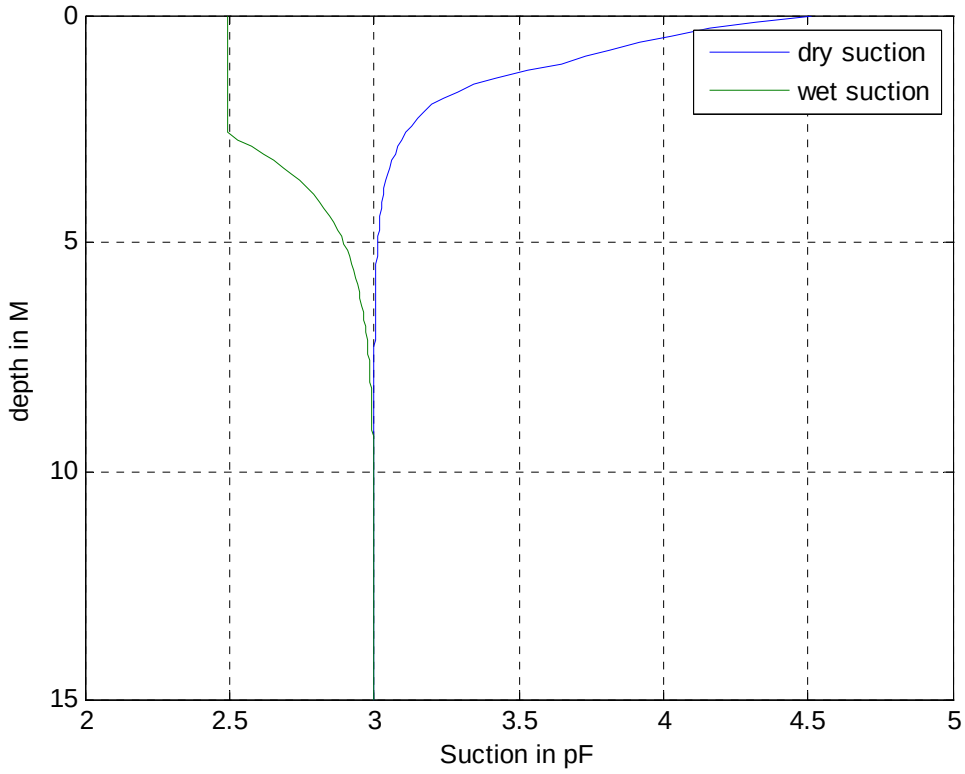

Fig.A-1. 1 Suction profile versus depth of slope.

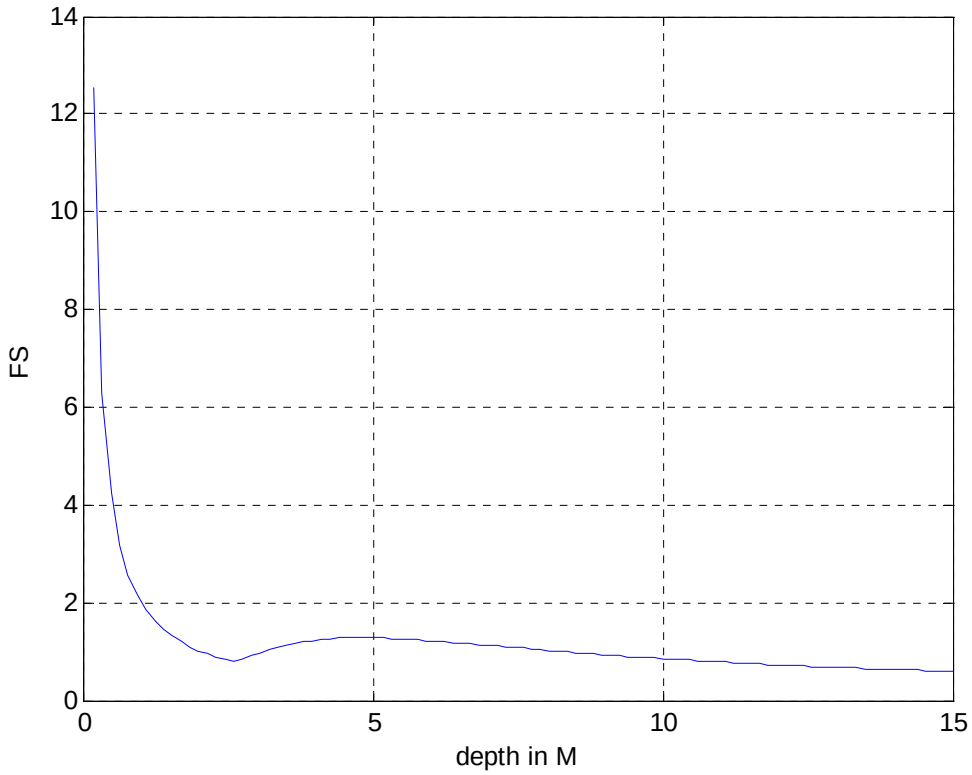

Fig.A-1 2 Factor of safety for slope versus depth of slope.

APPENDIX A-2

In this section, a program written in MATLAB® for generating correlation curve between suction and dielectric constant value. Input parameters for this program are as follows:

1. Dry unit weight of soil
2. Percent passing #200 sieve
3. Percent fine clay
4. Liquid limit of soil
5. Plasticity index of soil
6. Specific gravity of soil
7. Minimum and Maximum range of dielectric constant value for a given soil

MATLAB® program code

```
%program to find the strength due to suction from Dielectric constant
% Written by Vishal Dantal August 2009
clear all
%inputs
gD1= input('Enter dry unit weight in gm/cc  ') ; % dry unit weight in gm/cc
n = input('Enter #200 in percent for soil  ');% %passing through no 200 seive
pFC=input ('Enter amount of % Fine clay  '); % %fine clay
LL= input('Enter Liquid Limt for given soil  ');%liquid limit
```

```
PI= input('Enter Plasticity Index for given soil  ');%Plasticity Index
Gs= input('Enter Specific Gravity of soil  ');  % specific gravity
gW= 10; %unit weight of water in kN/m2
Es= 5;%input('Enter Dielectric constant for solid  '); % Dielectric constant for solid
Ew= 81; %Dielectric constant for water
Ea= 1; %Dielectric constant for air
Emin= input('Enter Dielectric constant for mix (min)  ') ; % Dielectric constant for mix
(min)
Emax= input('Enter Dielectric constant for mix (max)  '); % Dielectric constant for mix
(max)
Em=Emin;
gD=gD1*10;
Qs= gD/(Gs*gW);% volumetric soild content

% relationship between PI and phi'
phi =0.0028*(PI)^2-0.3487*(PI)+36.63;
phi1=(phi*pi/180);
pF0=5.622+0.0041*(pFC);
S=-20.29+0.1555*LL-0.117*PI+0.0684*(n);
% for loop
j=Emax-Emin;
for m=1:1+j
Em(m)=Emin+(m)-1;
Qw(m)=((sqrt(Em(m))-sqrt(Ea))-(sqrt(Es)-sqrt(Ea))*Qs)/(sqrt(Ew)-sqrt(Ea));
pF(m)=pF0-(abs(S)*gW*Qw(m)/gD);
Us(m)=0.09802 *10^(pF(m)); % Us= (Ua-Uw)
St(m)=Us(m)*Qw(m)*tan(phi1); % strength due to suction
end
```

```
Em1=transpose(Em);
St1=transpose(St);
pF1=transpose(pF);
plot (Em1,pF1);
xlabel('Dielectric constant of mix');
ylabel('pF');
```

Output for this program is as follows:

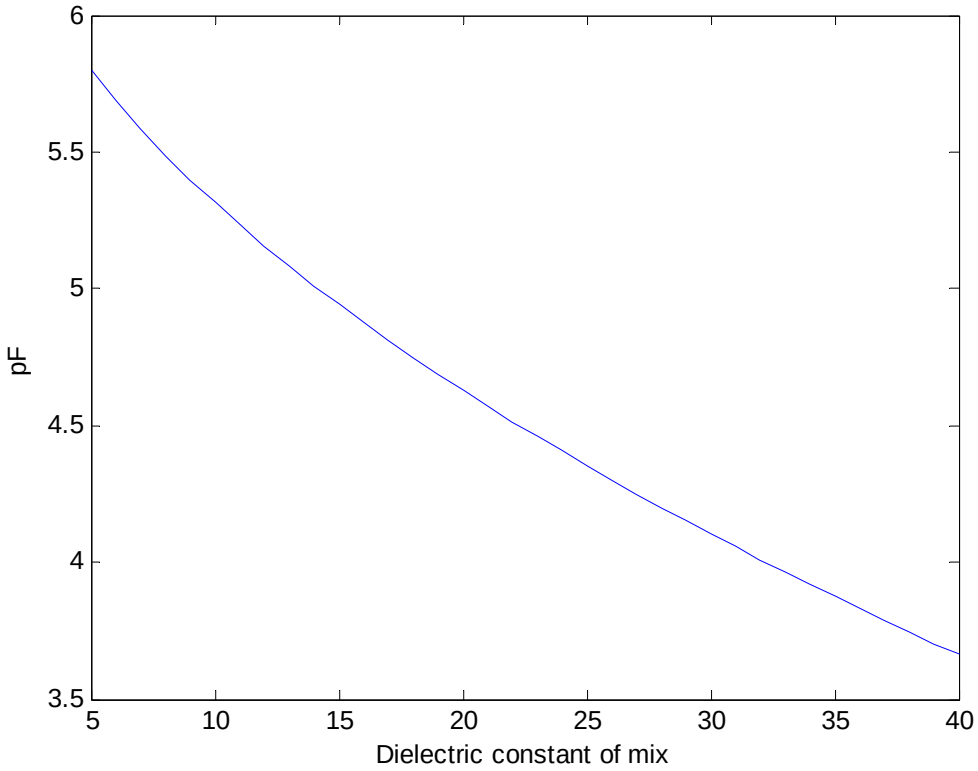

Fig.A-2. 1 Correlation between suction (pF) and dielectric constant of mix.

APPENDIX A-3

A Matlab® program for a parametric study is explained in this section. Inputs for this program are engineering properties of soil taken from the websoil survey web site.

MATLAB® program code

```
%program to find the strength due to suction from Dielectric constant
%For parametric study
% Written by Vishal Dantal. August-2009
clear all
%inputs
gt1= input('Enter bulk unit weight in gm/cc  ') ; % dry unit weight in gm/cc
w=input('Enter initial Voulmetic water content in %   ');% voulmetirc water content in %
n = input('Enter #200 in percent for soil  ');% %passing through no 200 seive
pFC=input ('Enter amount of % Fine clay  '); % %fine clay
LL= input('Enter Liquid Limt for given soil  ');%liquid limit
PI= input('Enter Plasticity Index for given soil  ');%Plasticity Index
Gs= 2.72;%input('Enter Specific Gravity of soil  ');  % specific gravity
gW= 10; %unit weight of water in kN/m2
Es= 5;%input('Enter Dielectric constant for solid  '); % Dielectric constant for solid
Ew= 81; %Dielectric constant for water
Ea= 1; %Dielectric constant for air
Emin= input('Enter Dielectric constant for mix (min)  ') ; % Dielectric constant for mix
(min)
Emax= input('Enter Dielectric constant for mix (max)  '); % Dielectric constant for mix
(max)
R=input('Enter the +/- range for curve   ');
Em=Emin;
```

```
gD1=gt1-(w/100)*gW/10;
gD=gD1*10;
Qs= gD/(Gs*gW);% volumetric soild content

% relationship between PI and phi'
phi =0.0028*(PI)^2-0.3487*(PI)+36.63;
phi1=(phi*pi/180);
pF0=5.622+0.0041*(pFC);
S=-20.29+0.1555*LL-0.117*PI+0.0684*(n);
% for loop
j=Emax-Emin;
for m=1:1+j
Em(m)=Emin+(m)-1;
Qw(m)=((sqrt(Em(m))-sqrt(Ea))-(sqrt(Es)-sqrt(Ea))*Qs)/(sqrt(Ew)-sqrt(Ea));
pF(m)=pF0-(abs(S)*gW*Qw(m)/gD);
pF2(m)=pF(m)+R;
pF3(m)=pF(m)-R;
Us(m)=0.09802 *10^(pF(m)); % Us= (Ua-Uw)
St(m)=Us(m)*Qw(m)*tan(phi1); % strength due to suction
%pF2
Us1(m)=0.09802 *10^(pF2(m));
St2(m)=Us1(m)*Qw(m)*tan(phi1);
%pF3
Us2(m)=0.09802 *10^(pF3(m));
St3(m)=Us2(m)*Qw(m)*tan(phi1);
end
Em1=transpose(Em);
```

```
St1=transpose(St);

St4=transpose(St2);
St5=transpose(St3);
pF1=transpose(pF);
pF4=transpose(pF2);
pF5=transpose(pF3);
plot(Em1,St4,'b',Em1,St1,'g',Em1,St5,'r');
xlabel('Dielectric constant of mix');
ylabel('Strength due to suction in kN/m2');
figure (2)
plot (Em1,pF4,'b',Em1,pF1,'g',Em1,pF5,'r');
xlabel('Dielectric constant of mix');
ylabel('pF');
```

Output of this program is

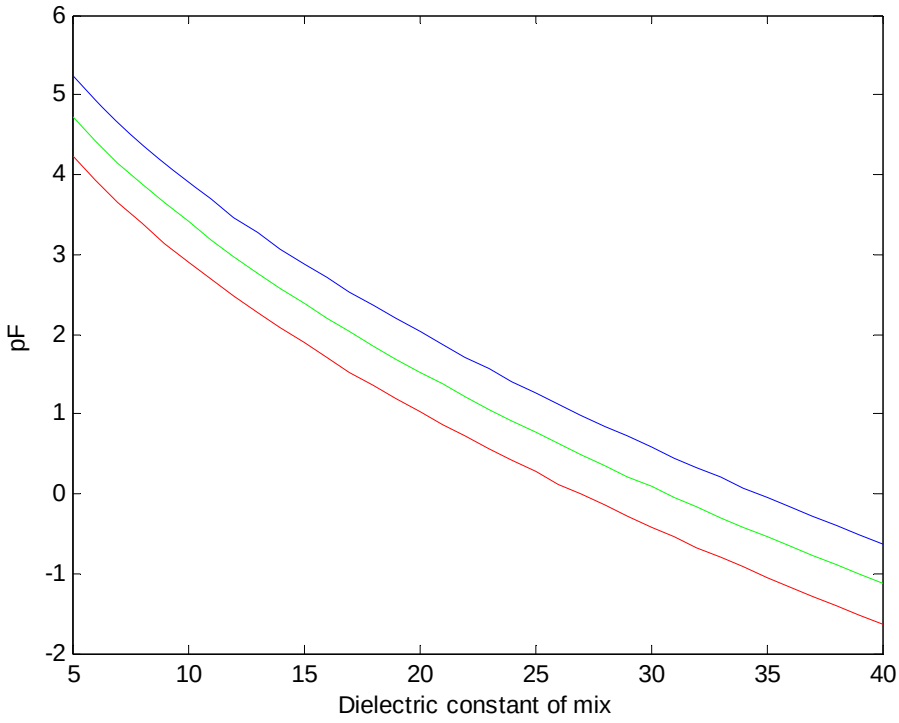

Fig.A-3. 1 Correlation curve between suction (pF) and dielectric constant value for parametric study.

APPENDIX B

Laboratory Data

For pure kaolinite.

water content calculation

Sample no	1	2	3	4	5	6
sample name	R-sp-1	M-sp-1	v-sp-1	v-sp-2	v-sp-3	V-Sp-5-1
Mass of Container Mc (gm)	1.03	1.01	1.01	1.02	1.01	22.34
Mc +wet mass of soil Mcws (gm)	21.56	21.88	26.46	29.02	18.66	30
Mc +dry mass of soil Mcs (gm)	15.99	16.79	19.37	21.2	13.46	28.51
Mass of water Mw (gm)	5.57	5.09	7.09	7.82	5.2	1.49
Mass of soil particles Ms (gm)	14.96	15.78	18.36	20.18	12.45	6.17
Moisture content % (Mw/Ms)	37.23262	32.25602	38.61656	38.75124	41.76707	24.14911
Emix (Dielectric constant value)	33.8	28.4	24.2	27.6	39.8	22.45
Temp C	22.3	23.1	23.7	23.7	23.2	23.2

Total unit weight calculations were performed on 5 samples and on one sample a compaction test was performed to make sample and to find dry density for that sample

Unit weight Calculation

Sample no	1			2			3			4			5		
Sample name	R-sp-1			M-sp-1			v-sp-1			vsp-2			v-sp-3		
trial	1	2	3	1	2	3	1	2	3	1	2	3	1	2	3
Diameter (mm)	77.74	72.72	77.45	69.96	75.83	75.58	50.81	50.31	51.42	51.61	52.23	50.12	49.86	50.68	50.49
Height (mm)	84.87	87.63	90.44	76.01	78.34	75.76	62.24	63.26	60.54	59.34	59.49	56.67	67.26	69.77	69.86
Volume (mm^3)	402841	363957	426082	292187	353798	339894	126200	125756	125718	124138	127460	111806	131326	140745	139871
Avg Volume (mm^3)	397626.64			328626.27			125890.99			121134.71			137314.10		
Mass (gm)	710.67			618.57			232.26			226.34			258.3		
total unit weight (gm/cc)	1.7873			1.8823			1.8449			1.8685			1.8811		
Moisture	0.372326203			0.322560203			0.386165577			0.387512389			0.417670683		

content w%					
Dry unit weight (gm/cc)	1.3024	1.4232	1.3310	1.3467	1.3269

From compaction test the dry unit weight of clay was g_d=12.61 kN/m^3 which is equal to 1.261 gm/cc and this was the sixth sample for clay (V-Sp-5-2)

After making samples and measuring moisture content for each sample, a filter paper test was conducted to find the suction value. Each sample was made into three small samples so as to get three trail points on suction test.

The results from filter paper test.

Total suction value trial point-1

Sample No:		1		2		3		4		5		6	
Sample Name		R-sp-1		M-sp-1		V-Sp-5-1		v-sp-1		v-sp-2		v-sp-3	
Moisture tin No		tu-1		tu-1				wd-1		wd-1		wd-1	
Total Suction													
Top or Bottom filter paper		T	B	T	B	T	B	T	B	T	B	T	B
Cold Tare Massg	Tc	30.977	30.922	30.651	30.587	31.1369	30.5113	31.2514	30.8186	30.8823	30.5441	31.3581	31.033
Mass of Wet paper + cold tare mass g	M1	31.227	31.184	30.925	30.856	31.3702	30.7469	31.5106	31.0667	31.1373	30.8018	31.6205	31.279
Mass of Dry paper + Hot tare mass g	M2	31.148	31.100	30.833	30.766	31.3143	30.6884	31.4304	30.9957	31.0538	30.7242	31.5338	31.199
Hot Tare mass g	Th	30.968	30.910	30.649	30.585	31.1315	30.5058	31.2489	30.8178	30.8748	30.539	31.3504	31.022
Mass of dry filter paper g (M2-Th)	Mf	0.179	0.190	0.184	0.181	0.1828	0.1826	0.1815	0.1779	0.179	0.1852	0.1834	0.1775
Mass of water in filter paper g (M1-M2-Tc+Th)	Mw	0.070	0.071	0.089	0.087	0.0505	0.053	0.0777	0.0702	0.076	0.0725	0.079	0.0686

Water content of filter paper g (Mw/Mf)	Wf	0.392	0.377	0.484	0.483	0.27626	0.29025	0.42810	0.39460	0.42458	0.39147	0.43075	0.38648
Avg water content	wf	0.3848		0.484		0.28326		0.41135		0.40802		0.40862	
Suction ,log kPa	h1	2.198	2.320	1.437	1.446	3.15500	3.03959	1.90277	2.17900	1.93178	2.20486	1.88088	2.24601
Suction ,pF	h2	3.198	3.320	2.437	2.446	4.15500	4.03959	2.90277	3.17900	2.93178	3.20486	2.88088	3.24601
Avg Suction, pF	h2	3.259		2.44176		4.09730		3.04088		3.06832		3.06345	

Total suction value trial point-2

Sample No:		1		2		3		4		5		6	
Sample Name		R-sp-1		M-sp-1		V-Sp-5-2		v-sp-1		v-sp-2		v-sp-3	
Moisture tin No		tu-2		tu-2				wd-2		wd-2		wd-2	
Total Suction													
Top or Bottom filter paper		T	B	T	B	T	B	T	B	T	B	T	B
Cold Tare Massg	Tc	30.520	30.433	30.792	30.520	30.555	30.753	30.668	31.496	30.422	30.426	30.6146	30.793
Mass of Wet paper + cold tare mass g	M1	30.773	30.701	31.044	30.7605	30.783	31.000	30.9376	31.7605	30.6716	30.682	30.8746	31.056

Mass of Dry paper + Hot tare mass g	M2	30.694	30.623	30.971	30.6884	30.724	30.937	30.8495	31.6755	30.601	30.606	30.7882	30.976
Hot Tare mass g	Th	30.517	30.431	30.786	30.5156	30.548	30.747	30.6585	31.4872	30.4194	30.423	30.6001	30.782
Mass of dry filter paper g (M2-Th)	Mf	0.1772	0.192	0.1848	0.1728	0.1762	0.19	0.191	0.1883	0.1816	0.1832	0.1881	0.1938
Mass of water in filter paper g (M1-M2-Tc+Th)	Mw	0.076	0.0763	0.0669	0.0672	0.0522	0.0567	0.0785	0.0757	0.0678	0.0727	0.0719	0.0688
Water content of filter paper g (Mw/Mf)	Wf	0.4288	0.3974	0.3620	0.38889	0.2962	0.2984	0.41099	0.40202	0.37335	0.3968	0.38224	0.3550
Avg water content	wf	0.41314		0.37545		0.29734		0.40651		0.38509		0.36862	
Suction ,log kPa	h1	1.8962	2.1559	2.4477	2.22613	2.9900	2.9722	2.04383	2.11786	2.35430	2.1606	2.28094	2.5055
Suction ,pF	h2	2.8962	3.1559	3.4477	3.22613	3.9900	3.9722	3.04383	3.11786	3.35430	3.1606	3.28094	3.5055
Avg Suction ,pF	h2	3.02609		3.33696		3.98116		3.08084		3.25745		3.39326	

Total suction value trial point-3

Sample No:		1		2		3		4		5	
Sample Name		R-sp-1		M-sp-1		v-sp-1		v-sp-2		v-sp-3	
Moisture tin No		tu-3		tu-3		wd-3		wd-3		wd-3	
Total Suction											
Top or Bottom filter paper		T	B	T	B	T	B	T	B	T	B
Cold Tare Massg	Tc	30.6564	30.7744	30.5458	30.767	30.6965	31.3809	30.9574	30.6641	30.8757	30.8528
Mass of Wet paper + cold tare mass g	M1	30.931	31.0484	30.794	31.0124	30.9545	31.6432	31.213	30.9067	31.1433	31.1168
Mass of Dry paper + Hot tare mass g	M2	30.8427	30.9507	30.7193	30.9428	30.8734	31.5642	31.1391	30.833	31.0541	31.0228
Hot Tare mass g	Th	30.6539	30.771	30.5391	30.761	30.6885	31.3737	30.9495	30.658	30.8673	30.8445
Mass of dry filter paper g (M2-Th)	Mf	0.1888	0.1797	0.1802	0.1818	0.1849	0.1905	0.1896	0.175	0.1868	0.1783
Mass of water in filter paper g (M1-M2-Tc+Th)	Mw	0.0858	0.0943	0.068	0.0636	0.0731	0.0718	0.066	0.0676	0.0808	0.0857

Water content of filter paper g (Mw/Mf)	Wf	0.45445	0.52476	0.37736	0.34983	0.39535	0.37690	0.34810	0.38629	0.43255	0.48065
Avg water content	wf	0.48961		0.36360		0.38613		0.36719		0.45660	
Suction ,log kPa	h1	1.68546	1.10558	2.32122	2.54821	2.17286	2.32498	2.56251	2.24760	1.86608	1.46937
Suction ,pF	h2	2.68546	2.10558	3.32122	3.54821	3.17286	3.32498	3.56251	3.24760	2.86608	2.46937
Avg Suction , pF	h2	2.39552		3.43472		3.24892		3.40506		2.66772	

Laboratory Data for normal soil

Sieve analysis data

The wet sieve analysis was done on this sample to get more accurate amount of fines present in this soil

Mechanical Analysis and Hydrometer for Silty Sand							
Total weight of sample (g):				500	Tested by: vishal dantal		
Hygroscopic water content (%):				0			
Total dry wieght of sample (g):				500.00			
Total weight of fine particles (g):				210.76			
Total weight of sand particles (g):				289.24			
Sieve No.	Size (mm)	Weight of Sieve (g)	Weight of Sieve + Soil (g)	Weight of Soil Retained (g)	Percent. Retained by Weight (%)	Percent. Accum. by Weight (%)	Percentage Passing by Weight (%)
10	2.00	605.30	605.40	0.10	0.02	0.02	99.98
20	0.90	368.20	368.50	0.30	0.06	0.08	99.92
40	0.43	344.30	348.90	4.60	0.92	1.00	99.00
80	0.18	316.80	486.50	169.70	33.92	34.91	65.09
200	0.075	340.90	449.60	108.70	21.72	56.64	43.36
Pan		477.70	483.90	216.96	43.36	100.00	0.00

Total Weight of Soil (g) =	500.36	100.00		
Percentage Error (%) =	0.07	< 2% O.K.		
Total Percent of Particles Passing Seive # 200 (%) =	43.36			

Hydrometer Analysis										
Hygroscopic Water Content										
1) Cup No. :			1			2) Mass of cup (g):			22.85	
3) Mass cup + soil (air dry) (g):			39.41			4) Mass cup + soil (oven dry) (g):			39.08	
5) Mass of water (g):			0.33			6) Mass of soil (oven dry) (g):			16.23	
7) Mass of soil (air dry) (g):			16.56			8) Hygrosc. water content (%):			2.03	
9) Hygrosc. correction factor:			1.000							
Hydrometer Analysis										
Hydrometer Type:			151 H			Specific Gravity:		2.67		
Hydrometer Reading in the Control Solution:			1.002			Calculate mass of oven dry soil:		0.00		
Mass of air dry soil:			50			Starting Time:		13:30:00		
Date	**Time**	**Elapsed Time (min)**	**Actual Hydrometer Reading (Rh)**	**Composite Correction**	**Hydrometer Reading Correction (Rh)**	**Temperature (Degrees C)**	**Effective Hydrometer Depth (L)**	**K from table**	**Diameter of Particle, D (mm)**	**Percent finer in suspension (%)**

8/12/2009	13:30:04	0.07	1.0155	0.0020	1.0135	26.0	12.18	0.012644	0.17093	33.64
8/12/2009	13:30:15	0.25	1.0145	0.0020	1.0125	26.0	12.45	0.012644	0.08922	30.43
8/12/2009	13:30:30	0.50	1.0135	0.0020	1.0115	26.0	12.71	0.012644	0.06375	27.23
8/12/2009	13:31:00	1.00	1.0125	0.0020	1.0105	26.0	12.97	0.012644	0.04554	24.03
8/12/2009	13:31:30	1.50	1.0122	0.0020	1.0102	26.0	13.07	0.012644	0.03732	22.90
8/12/2009	13:32:00	2.00	1.0121	0.0020	1.0101	26.0	13.09	0.012644	0.03235	22.58
8/12/2009	13:35:00	5.00	1.0115	0.0020	1.0095	26.0	13.24	0.012644	0.02057	20.82
8/12/2009	13:45:00	15.00	1.0110	0.0020	1.0090	26.0	13.37	0.012644	0.01194	19.22
8/12/2009	14:00:00	30.00	1.0110	0.0020	1.0090	26.0	13.37	0.012644	0.00844	19.22
8/12/2009	14:30:0	60.00	1.0110	0.0020	1.0090	26.0	13.37	0.01264	0.00597	19.22

8/12/2009	15:00:00	90.00	1.0108	0.0020	1.0088	26.0	13.44	0.012644	0.00489	18.42
8/12/2009	15:30:00	120.00	1.0100	0.0020	1.0080	26.0	13.63	0.012644	0.00426	16.02
8/12/2009	8:30:00	1140.00	1.0100	0.0020	1.0080	26.0	13.63	0.012644	0.00138	16.02
8/13/2009	15:45:00	1440.00	1.0100	0.0020	1.0080	26.0	13.63	0.012644	0.00123	16.02

Atterberg limits

Liquid Limit test				
Sample no	1	2	3	4
Mass of Container Mc (gm)	1.02	1	1.02	1.01
Mc +wet mass of soil Mcws (gm)	13.37	19.12	17.79	20.43
Mc +dry mass of soil Mcs (gm)	10.1	14.4	13.47	15.65
Mass of water Mw (gm)	3.27	4.72	4.32	4.78
Mass of soil particles Ms (gm)	9.08	13.4	12.45	14.64
Moisture content % (Mw/Ms)	36.01322	35.22388	34.6988	32.65027
No drops	18	23	28	37

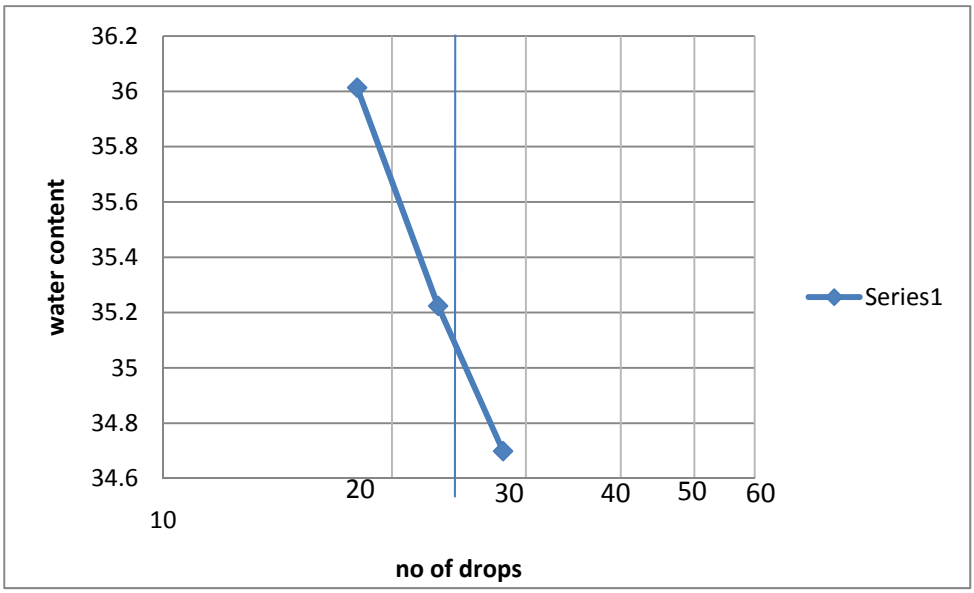

Plastic limit test

Sample no	1	3		
Mass of Container Mc (gm)	22.27	22.32		
Mc +wet mass of soil Mcws (gm)	28.47	28.41		
Mc +dry mass of soil Mcs (gm)	27.65	27.63		
Mass of water Mw (gm)	0.82	0.78		
Mass of soil particles Ms (gm)	5.38	5.31		
Moisture content % (Mw/Ms)	15.24164	14.68927		
Avg	14.96545			

Compaction test

In this test, a standard proctor compaction method was used to make samples for filter paper test.

Sr No	Mass of mold + moist soil Msm (kg)	Mass of Mold Mm (kg)	Mass of moist soil Mt (kg)	Volume of mold (m3)	unit weight of soil gt (kN/m3)	Water content Determination							Dry unit weight of soil gd (kN/m3)
						Can No	Mass of Can Mc (g)	Mass of wet soil + Can Msc (g)	Mass of Dried soil +Can Msc (g)	Mass of Water Mw (g)	Mass of Dry soil Ms (g)	water Content w (%)	
1	4.13241	2.38422	1.74819	0.000944	18.5180	1	20.79	63.29	55.31	7.98	34.52	23.11703	15.0410
2	4.33169	2.38631	1.94538	0.000944	20.6070	2	22.2	53.62	48.68	4.94	26.48	18.65559	17.3670
3	4.36874	2.38634	1.9824	0.000944	21	3	22.28	58.94	53.72	5.22	31.44	16.60305	18.0090
4	4.3672	2.38723	1.97997	0.000944	20.9740	4	22.19	47.79	44.58	3.21	22.39	14.33676	18.3440
5	4.27367	2.38738	1.88629	0.000944	19.9810	5	22.01	57.9	54.07	3.83	32.06	11.94635	17.8490

Water content calculation and measuring dielectric constant value for sample.

water content calculation

Sample no	1	2	3	4	5
sample name	V-sand-1	V-sand-2	V-sand-3	V-sand-4	V-sand-5
Mass of Container Mc (gm)	20.79	22.2	22.19	22.28	22.01
Mc +wet mass of soil Mcws (gm)	63.29	53.62	47.79	58.94	57.9
Mc +dry mass of soil Mcs (gm)	55.31	48.68	44.58	53.72	54.07
Mass of water Mw (gm)	7.98	4.94	3.21	5.22	3.83
Mass of soil particles Ms (gm)	34.52	26.48	22.39	31.44	32.06
Moisture content % (Mw/Ms)	23.11703	18.65559	14.33676	16.60305	11.94635
Emix	39.4	30	21.5	24.7	19.8
Temp C	20.8	23.9	23.4	23.2	23.4

Total suction value from filter paper test trial point-1

Sample No:		1		2		3		4		5	
Sample Name		V-sand-1		V-sand-2		V-sand-3		V-sand-4		V-sand-5	
Moisture tin No		9	17	33	22	36	22	19	23	32	29
Top or Bottom filter paper		T	B	T	B	T	B	T	B	T	B
Cold Tare Massg	Tc	30.547	30.510	30.632	30.739	31.168	30.739	30.752	30.598	30.6886	30.3529
Mass of Wet paper + cold tare mass g	M1	30.800	30.772	30.877	30.993	31.427	30.974	31.005	30.843	30.9353	30.5957
Mass of Dry paper + Hot tare mass g	M2	30.721	30.686	30.800	30.921	31.344	30.904	30.930	30.772	30.8626	30.5195
Hot Tare mass g	Th	30.543	30.503	30.624	30.737	31.159	30.732	30.746	30.594	30.6827	30.3424
Mass of dry filter paper g (M2-Th)	Mf	0.1779	0.1832	0.1753	0.1834	0.1847	0.1715	0.1839	0.1773	0.1799	0.1771
Mass of water in filter paper g	Mw	0.076	0.0782	0.0692	0.0705	0.0751	0.0638	0.0691	0.0673	0.0668	0.0657

Water content of filter paper g	Wf	0.4272	0.4268	0.3947	0.3844	0.4066	0.3720	0.3757	0.3795	0.37132	0.37098
Avg Water content	wf	0.42703		0.38958		0.38931		0.37767		0.37115	
Suction ,log kPa	h1	1.9014	1.9043	2.1690	2.2544	2.0713	2.3566	2.3258	2.2941	2.36235	2.36515
Suction ,pF	h2	2.9014	2.9043	3.1690	3.2544	3.0713	3.3566	3.3258	3.2941	3.36235	3.36515
Avg Suction ,pF	h2	2.90287		3.21174		3.21397		3.31000		3.36375	

Total suction value from filter paper test trial point-2

Sample No:		1		2		3		4		5	
Sample Name		V-Sand-1		V-Sand-2		V-Sand-3		V-Sand-4		V-Sand-5	
Moisture tin No		23	21	29	28	13	9	24	34	21	28
Top or Bottom filter paper		T	B	T	B	T	B	T	B	T	B
Cold Tare Massg	Tc	30.598	30.514	30.356	30.366	30.326	30.549	30.307	30.442	30.512	30.3672
Mass of Wet paper	M1	30.850	30.752	30.608	30.622	30.571	30.781	30.559	30.685	30.7518	30.6002

Mass of Dry paper + Hot tare mass g	M2	30.773	30.680	30.526	30.548	30.501	30.717	30.486	30.604	30.6796	30.5282
Hot Tare mass g	Th	30.592	30.508	30.344	30.363	30.321	30.546	30.303	30.431	30.5032	30.3569
Mass of dry filter paper g	Mf	0.181	0.1724	0.1813	0.1853	0.18	0.1713	0.1836	0.1732	0.1764	0.1713
Mass of water in filter paper g	Mw	0.0703	0.0653	0.0705	0.071	0.0651	0.0612	0.0681	0.0699	0.0634	0.0617
Water content of filter paper g	Wf	0.3884	0.3787	0.3888	0.3831	0.3616	0.3572	0.3709	0.4035	0.35941	0.36019
Avg Water content	wf	0.38358		0.38601		0.35947		0.38725		0.35980	
Suction ,log kPa	h1	2.2214	2.3008	2.2176	2.2646	2.4419	2.4782	2.3656	2.0962	2.46054	2.45414
Suction ,pF	h2	3.2214	3.3008	3.2176	3.2646	3.4419	3.4782	3.3656	3.0962	3.46054	3.45414
Avg Suction ,pF	h2	3.26118		3.24117		3.46007		3.23097		3.45734	

APPENDIX C

THE FILTER PAPER METHOD FOR TOTAL AND MATRIC SUCTION MEASUREMENTS

The procedure for measuring suction through filter paper test is explained in this appendix. The procedure in this appendix is used from the TxDot report No: FHWA/TX-05/0-4518-1 and the title of the report is Design Procedure for Pavements on Expansive Soils Volume-2 Appendix-A

OVERVIEW

This procedure determines the soil total and matric suction components using the filter paper method. The procedure uses the wetting filter paper calibration curve developed in the (Bulut et al. 2001) paper for both total and matric suction components. The wetting filter paper calibration curve was constructed for Schleicher & Schuell No. 589-White Hard (WH) 5.5 cm in diameter filter papers. Thus, the same brand of filter paper must be adopted for both total and matric soil suction measurements.

Basically, the filter paper comes to equilibrium with the soil either through vapor (total suction measurement) or liquid (matric suction measurement) flow. At equilibrium, the suction value of the filter paper and the soil will be equal. After equilibrium is established between the filter paper and the soil, the water content of the filter paper disc is measured. Then, by using the wetting filter paper calibration curve, the corresponding suction value is found from the curve.

Before commencing the soil suction measurements, carefully clean all the items related to filter paper testing. Use latex gloves and tweezers to handle the materials in nearly all steps of the experiment. The filter papers and aluminum cans for water content measurements are never touched with bare hands. In addition, it is suggested that two persons perform the filter paper water content measurements in order to reduce the time during which the filter papers are exposed to the laboratory atmosphere and, thus, the amount of moisture lost or gained during measurements is kept to a minimum.

DEFINITIONS

The following definitions are referenced in this test method:

- Total suction – total suction is expressed in log kPa or pF scales, and is the equivalent suction derived from the measurement of the partial pressure of the water vapor in equilibrium with the soil water, relative to the partial pressure of water vapor in equilibrium with free pure water.
- Matric suction – matric suction is expressed in log kPa or pF scales, and is the equivalent suction derived from the measurement of the partial pressure of the water vapor in equilibrium with the soil water, relative to the partial pressure of the water vapor in equilibrium with a solution identical in composition with the soil water.
- Wetting filter paper calibration curve – the calibration curve adopted for this procedure is obtained from initially dry filter papers that are held over salt solutions, in a non-contact manner, at isothermal conditions.

- Suction in pF – suction in pF scale is expressed as pF = log10 (suction in cm of water).
- Suction in log kPa – suction in log kPa scale is expressed as log kPa ≈pF – 1.

APPARATUS

The following apparatus is required:

- Schleicher & Schuell No. 589-White Hard quantitative 5.5 cm in diameter filter papers.
- Sensitive balance, with 0.0001 grams accuracy.
- Constant temperature environment, with stability in temperature less than ±1 ^{o}C, preferably in the order of ±0.1 ^{o}C.
- Oven for 110 ±5 ^{o}C.
- Glass jars; glass jars that are between 250 to 500 ml volume sizes are readily available in the market and can be easily adopted for suction measurements. Glass jars, especially, with 3.5 to 4 inch (8.89 to 10.16 cm) diameter can contain the 3 inch (7.62 cm) diameter Shelby tube samples very nicely.
- Protective filter papers; filter papers of any brand that are larger in diameter than the 5.5 cm diameter Schleicher & Schuell No. 589-WH filter papers can be employed as protective filter papers for relatively wet soil samples during matric

suction measurements. Filter papers that are 7 cm in diameter are available in the market and are ideal for Shelby tube soil sample sizes.

- Moisture tins for the filter paper water content determination.
- Ring type support; a ring support that has a diameter smaller than filter paper diameter and in between 1.5 to 2 cm in height. Care must be taken when selecting the support material; materials that can corrode should be avoided, plastic or glass type materials are much better for this job. The PVC pipes work nicely for this purpose.
- Aluminum block; an aluminum block functions as a heat sink and expedites the cooling of the hot moisture tins.
- Ice chests, tweezers, scissors, latex gloves, electrical tape, knives, spatula, etc.

PROCEDURE FOR TOTAL SUCTION MEASUREMENTS

The following steps are necessary to determine total suction.

1. Cut and trim the soil specimen with minimum disturbance into right circular cylinder (see Figure C-1), if possible, to fit into the glass jar.
2. Fill at least 75 percent by volume of the glass jar with the soil; the smaller the empty space remaining in the glass jar, the smaller the time period that the filter paper and the soil system requires to come to equilibrium, and also the smaller the change in the soil specimen water content as a result of the release of water vapor into the empty space in the jar.

3. Put a ring-type support on top of the soil to provide a non-contact system between the filter paper and the soil.
4. Insert two Schleicher & Schuell No. 589-WH filter papers one on top of the other on the ring using tweezers. The filter papers should not touch the soil, the inside wall of the jar, or underneath the lid in any way.
5. Seal the glass jar lid very tightly with electrical tape.
6. Repeat steps 1 through 5 for every soil specimen.
7. Carry the glass jars very carefully to the ice chests in a temperature controlled room for equilibrium.

After an equilibration time of at least one week in the temperature-controlled room, the procedure for the filter paper water content measurements is as follows:

1. Before removing the glass jars from the temperature-controlled room, weigh all aluminum cans that are used for moisture content measurements to the nearest 0.0001 g accuracy as *cold tare mass (Tc)* and record in Table C-1.
2. Remove a glass jar from the ice chest in the temperature-controlled room.
3. Carry out all measurements by two persons. For example, while one person is opening the sealed glass jar, the other is putting the filter paper into the aluminum can very quickly (i.e., in a few seconds) using tweezers.

4. Take the weights of each can with wet filter paper inside very quickly and record as *mass of wet filter paper + cold tare mass (M1)* in the corresponding space in Table C-1, and marked whether it is a top or bottom filter paper.
5. Record the other relevant information (such as the moisture tin number, depth, etc.) on the sheet.
6. Follow steps 2 through 5 for every glass jar.
7. Put all cans into the oven with the lids half-open to allow evaporation.

Keep all filter papers at 110 ±5 ^{o}C temperature inside the oven for at least 10 hrs. Before taking measurements of the dried filter papers, close the cans with their lids and allow to equilibrate for about 5 minutes inside the oven.

1. Remove a can from the oven and put it on an aluminum block (i.e., heat sinker) for about 20 seconds to cool down.
2. Weigh the can with the dry filter paper inside very quickly and record as *mass of dry filter paper + hot tare mass (M2)* in Table C-1.
3. Take the dry filter paper from the can and weigh the cooled can again in a few seconds and record as *hot tare mass (Th)* in Table C-1.
4. Repeat steps 1 through 3 for every can.

- Calculations

The filter paper water contents for obtaining total suctions are calculated as follows (see Table C-1).

1. Mass of dry filter paper, $M_f = M_2 - T_h$
2. Mass of water in filter paper, $M_w = M_1 - M_2 - T_c + T_h$
3. Filter paper water content, $W_f = M_w / M_f$
4. Repeat steps 1, 2, and 3 for every filter paper.

After obtaining all of the filter paper water contents, the equation for the wetting filter paper calibration curve (Figure C-2) is employed to get total suction values of the soil samples.

$h_1 = -8.247W_f + 5.4246$ ($h_1 > 1.5$ log kPa)

where:

h_1 = total suction (in log kPa)

W_f = filter paper water content (in decimals)

And

$h_2 = -8.247W_f + 6.4246$ (h2 > 2.5 pF)

where:

h_2 = total suction (in pF)

- Reporting Test Results

Total suction values are reported to the nearest two decimal places in log kPa or pF scales.

PROCEDURE FOR MATRIC SUCTION MEASUREMENTS

Soil matric suction measurements are very similar to the total suction measurements except instead of inserting filter papers in a non-contact manner with the soil for total suction testing, a good intimate contact should be provided between the filter paper and the soil for matric suction measurements. Both matric and total suction measurements can be performed on the same soil sample in a glass jar as shown in Figure C-1.

The following steps are necessary to determine matric suction:

1. Cut and trim the soil specimen with minimum disturbance into two right circular cylinders (see Figure C-1), if possible, that can fit into the glass jar.
2. Sandwich a Schleicher & Schuell No. 589-WH 5.5 cm in diameter filter paper between two larger diameter protective filter papers.
3. Insert the sandwiched filter papers into the soil sample in a very good contact manner. An intimate contact between the filter paper and the soil is very important.
4. Bring the two halves of the cylindrical samples together and seal with electrical tape to keep the two specimens together in a good contact manner.
5. Put the whole sample with embedded filter papers into the glass jar container. Fill at least 75 percent by volume of the glass jar with the soil; the smaller the empty space remaining in the glass jar, the smaller the change in the soil

specimen water content as a result of the release of water vapor into the empty space in the jar.

NOTE: The same soil sample can be used to infer both total and matric suction.

6. Seal the glass jar lid very tightly with electrical tape.
7. Repeat steps 1 through 6 for every soil specimen.
8. Carry the glass jars very carefully to the ice chests in a temperature controlled room for equilibrium.

After an equilibration time of at least one week in the temperature-controlled room, the procedure for the filter paper water content measurements is as follows:

1. Before removing the glass jars from the temperature-controlled room, weigh all aluminum cans that are used for moisture content measurements to the nearest 0.0001 g accuracy as *cold tare mass (Tc)* and recorded in Table C-1.
2. Remove a glass jar from the ice chest in the temperature-controlled room.
3. After that, carry out all measurements by two persons. For example, while one person is opening the sealed glass jar, the other is putting the filter paper into the aluminum can very quickly (i.e., in a few seconds) using tweezers.
4. Take the weights of each can with wet filter paper inside very quickly and record as *mass of wet filter paper + cold tare mass (M1)* in the corresponding space in Table C-1, and mark as matric suction.

5. Record the other relevant information (such as the moisture tin number, depth, etc.) on the sheet.
6. Repeat steps 2 through 5 for every glass jar.
7. Put all cans into the oven with the lids half-open to allow evaporation.

Keep all filter papers at 110 ±5 oC temperature inside the oven for at least 10 hrs. Before taking measurements on the dried filter papers close the cans with their lids and allow to equilibrate for about 5 minutes inside the oven.

1. Remove a can from the oven and put it on an aluminum block (i.e., heat sinker) for about 20 seconds to cool down.
2. Weigh the can with the dry filter paper inside very quickly and record as *mass of dry filter paper + hot tare mass (M2)* in Table C-1.
3. Take the dry filter paper from the can and weigh the cooled empty can again in a few seconds and record as *hot tare mass (Th)* in Table C-1.
4. Repeat steps 1 through 3 for every can.

- Calculations

The filter paper water contents for obtaining matric suctions are calculated as follows (see Table C-1).

1. Mass of dry filter paper, $M_f = M_2 - T_h$
2. Mass of water in filter paper, $M_w = M_1 - M_2 - T_c + T_h$

3. Filter paper water content, $W_f = M_w / M_f$

4. Repeat steps 1, 2, and 3 for every filter paper.

After obtaining all of the filter paper water contents, the equation for the wetting filter paper calibration curve (Figure C-2) is employed to get matric suction values of the soil samples.

$h_1 = -8.247W_f + 5.4246$ ($h_1 > 1.5$ log kPa)

where:

h_1 = matric suction (in log kPa)

W_f = filter paper water content (in decimals)

and

$h_2 = -8.247W_f + 6.4246$ ($h_2 > 2.5$ pF)

where:

h2 = matric suction (in pF)

- Reporting Test Results

Matric suction values are reported to the nearest two decimal places in log kPa or pF scales.

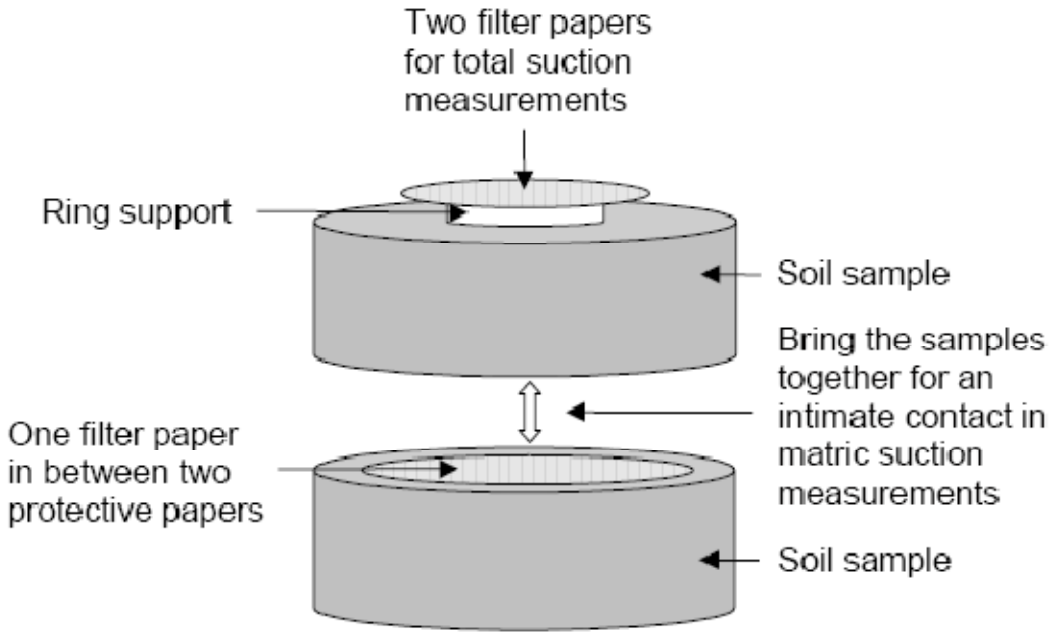

Fig.C. 1 Total and matric suction measurements(Bulut et al. 2001).

Table C. 1 The filter paper method suction measurements worksheet

THE FILTER PAPER METHOD SUCTION MEASUREMENTS WORKSHEET									
Date Sampled:								Date Tested:	
Boring No.:								Tested By:	
Sample No.:									
Depth									
Moisture Tin No.:									
Total or Matric Suction									
Top or Bottom Filter Paper									
Cold tare mass, g	T_c								
Mass of wet filter paper + cold tare mass, g	M_1								
Mass of dry filter paper + hot tare mass, g	M_2								
Hot tare mass, g	T_h								
Mass of dry filter paper, g ($M_2 - T_h$)	M_f								
Mass of water in filter paper, g ($M_1 - M_2 - T_c + T_h$)	M_w								
Water content of filter paper, g (M_w / M_f)	W_f								
Suction, log kPa	h_1								
Suction, pF	h_2								

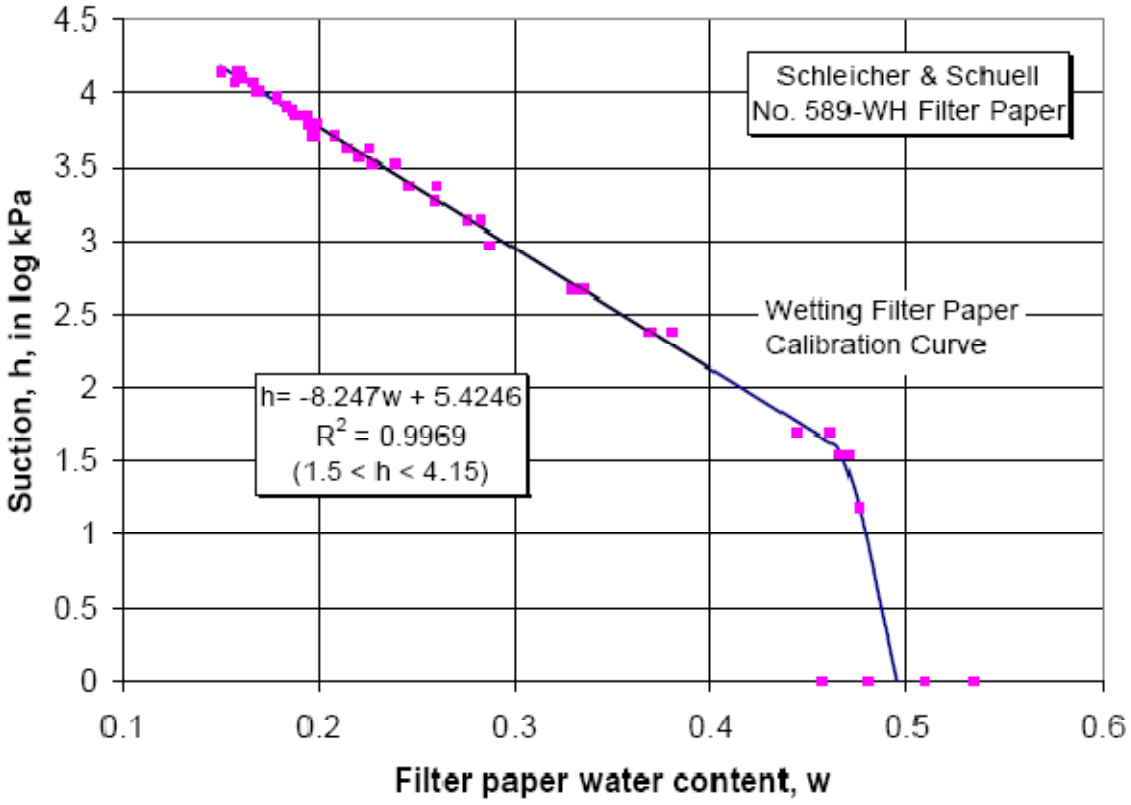

Fig.C. 2 Filter paper calibration curve(Bulut et al. 2001).

VITA

Name: Vishal Dantal

Address: Department of Civil Engineering, Texas A&M University
3136 TAMU, College Station, TX-77843-3136

Email Address: vishaldantal@tamu.edu

Education: B.E., Sadar Patel College of Engineering, Mumbai, India, 2006
M.S., Civil Engineering, Texas A&M University, 2009